An effective fragment method for modeling solvent effects in quantum mechanical calculations

Paul N. Day, Jan H. Jensen, Mark S. Gordon, Simon P. Webb, Walter J. Stevens, Morris Krauss, David Garmer, Harold Basch, and Drora Cohen

Citation: The Journal of Chemical Physics **105**, 1968 (1996); doi: 10.1063/1.472045
View online: http://dx.doi.org/10.1063/1.472045
View Table of Contents: http://scitation.aip.org/content/aip/journal/jcp/105/5?ver=pdfcov
Published by the AIP Publishing

Articles you may be interested in

The effective fragment model for solvation: Internal rotation in formamide
J. Chem. Phys. **105**, 11081 (1996); 10.1063/1.472909

Development and validation of reliable quantum mechanical approaches for the study of free radicals in solution
J. Chem. Phys. **105**, 11060 (1996); 10.1063/1.472906

An ab initio study of solvent shifts in vibrational spectra
J. Chem. Phys. **105**, 2961 (1996); 10.1063/1.472169

Solvent effects on the potential energy surface of the 1:1 complex of water and formamide: Application of the polarizable continuum model to the study of nonadditive effects
J. Chem. Phys. **104**, 5539 (1996); 10.1063/1.471793

The structures and conformations of lithium-aza-enolates of peptides: What do semiempirical and ab initio calculations predict?
AIP Conf. Proc. **330**, 238 (1995); 10.1063/1.47694

This article is copyrighted as indicated in the article. Reuse of AIP content is subject to the terms at: http://scitation.aip.org/termsconditions. Downloaded to IP: 128.231.128.169 On: Mon, 07 Dec 2015 18:36:59

An effective fragment method for modeling solvent effects in quantum mechanical calculations

Paul N. Day,[a] Jan H. Jensen, Mark S. Gordon, and Simon P. Webb
Department of Chemistry, Iowa State University, Ames, Iowa 50011

Walter J. Stevens and Morris Krauss
Center for Advanced Research in Biotechnology, National Institute of Standards and Technology, and University of Maryland Biotechnology Institute, 9600 Gudelsky Drive, Rockville, Maryland 20850

David Garmer
Department of Physiology and Biophysics, Mt. Sinai Medical Center, New York, New York 10029

Harold Basch and Drora Cohen
Chemistry Department, Bar Ilan University, Ramat Gan 52100, Israel

(Received 14 December 1995; accepted 19 April 1996)

An effective fragment model is developed to treat solvent effects on chemical properties and reactions. The solvent, which might consist of discrete water molecules, protein, or other material, is treated explicitly using a model potential that incorporates electrostatics, polarization, and exchange repulsion effects. The solute, which one can most generally envision as including some number of solvent molecules as well, is treated in a fully *ab initio* manner, using an appropriate level of electronic structure theory. In addition to the fragment model itself, formulae are presented that permit the determination of analytic energy gradients and, therefore, numerically determined energy second derivatives (hessians) for the complete system. Initial tests of the model for the water dimer and water-formamide are in good agreement with fully *ab initio* calculations. © *1996 American Institute of Physics.* [S0021-9606(96)02428-2]

I. INTRODUCTION

The vast majority of chemical processes occur in solution, on surfaces, and at the active sites of enzymes. Therefore, the development of predictive quantum chemistry-based methods to study conformational energetics, molecular stabilities, electronic properties, and chemical reactivities, and dynamical behavior of molecules in the condensed phase is a high priority. Several approaches for treating processes in solution using quantum chemistry have been proposed. Currently, the most widely used methods employ a continuum treatment of the bulk solvent through the quantum mechanical implementation of Onsager's reaction field model[1] via a modified molecular Hamiltonian that couples the electric field of the solute molecule to the bulk polarizability of the solvent.[2–5] The quantum mechanical implementation commonly involves a bulk dielectric constant for the solvent and a spherical or elipsoidal cavity surrounding the solute molecule. More sophisticated methods use more complex cavity shapes.[6] Other condensed-phase methods use more structured approaches that account for the influence of surrounding ''perturber'' molecules by introducing point charges[7] or a combination of point charges and atomic polarizabilities[8] into the Hamiltonian of the molecule being treated quantum mechanically. Warshel and co-workers[9] have developed methods which include the dynamical effects of nearby solvent molecules through a Langevin dipole formalism. Recently, several groups have introduced hybrid methods which couple quantum mechanical calculations to molecular dynamics using either classical force fields for large systems[10] or quantum mechanical forces for small clusters.[11]

In this paper, we present an *ab initio* computational approach[12] to describing molecular systems in the presence of nonbonded, perturbing solvent molecules. The method, which is in the spirit of earlier work by Förner and co-workers,[13] Ohta, *et al.*[14] and recently discussed by van Duijnen and co-workers,[15] makes use of perturbing Hamiltonians that are referred to as *effective fragment potentials* (EFP). These potentials, firmly based in quantum mechanics, are intended to replace molecules or molecular fragments in *ab initio* electronic structure calculations, and thus allow the use of larger and more realistic model systems in the study of condensed phase chemistry, molecular interactions at surfaces, or enzymatic reaction mechanisms. In their present form, the EFP's simulate the most important nonbonded energy terms in van der Waals or hydrogen bonded complexes, including Coulomb interactions, polarization, and exchange repulsion. The EFP's are used to replace one or more ''*spectator*'' molecules (e.g., solvent) in complex systems in order to investigate the properties of ''*active*'' molecules (e.g., solute) in the presence of the perturbing spectators. Comparison with past efforts of this general type will be made as appropriate in the discussion below. A potential extension of this method is the subdivision of a single molecular species (e.g., a polymer) into ''active'' and ''spectator'' fragments.

In the EFP model, the electrostatic potential of a spectator molecule is included as a one-electron term in the quantum mechanical Hamiltonian of the active part of the system.

[a]Current address: MLPJ, Materials Directorate, Wright Laboratory, Wright-Patterson Air Force Base, Ohio 45433.

 0021-9606/96/105(5)/1968/19/$10.00 © 1996 American Institute of Physics
This article is copyrighted as indicated in the article. Reuse of AIP content is subject to the terms at: http://scitation.aip.org/termsconditions. Downloaded to IP: 128.231.128.169 On: Mon, 07 Dec 2015 18:36:59

An accurate, but relatively compact, representation of the electrostatic potential in the important interaction regions is achieved using a distributed multipolar analysis (DMA) of the spectator charge distributions[16,17] multiplied by distance-dependent cutoff functions to account for charge penetration effects. The polarization of the spectator molecules by the electric field of the active molecules is treated by a self-consistent perturbation model employing bond and lone pair dipole polarizabilities extracted from finite-field perturbed Hartree–Fock calculations on isolated spectator molecules.[18] The exchange repulsion between the active and spectator molecules is also modeled by one-electron terms in the active-space Hamiltonian that have the form of simple Gaussian functions located at the spectator atom centers. The Gaussian functions are optimized by fitting interaction energy components of prototypical complexes.

A prime motivation for the development of the effective fragment method as outlined above and detailed below has been its firm foundation in quantum mechanics. The Hamiltonian used to describe the system embodies the essential physics. Consequently, there is a clear path for systematically improving the model by removing the approximations invoked in its implementation.

The methods used to construct each of the EFP components are described below, along with the results of various test calculations that are compared to *ab initio* data obtained from reduced variational space (RVS)[19] decompositions of molecular interaction energies into electrostatic, polarization, and exchange-repulsion contributions.

The remaining intermolecular interactions that are not currently addressed in the EFP approach are charge transfer, dispersion, and other interactions occurring at higher orders in perturbation theory. The energetics of these extra components may be treated by explicit nonquantum mechanical atom–atom force fields or by adjustment of the repulsive potentials as discussed below.

The formalism to permit relaxation of the positions and orientations of the fragments relative to the solute is also developed in this paper. The effective fragment potential is then used to find the minimum energy geometry of test solute–solvent (active-spectator) systems.

II. ELECTROSTATIC INTERACTIONS

A. Distributed multipoles

The electrostatic interaction between two polar molecules often dominates the total interaction energy and accounts for a large part of the anisotropy of the interaction energy surface.[20] Methods for the inclusion of external electrostatic perturbations in quantum mechanical calculations have been developed previously.[7] Atom-centered fractional charges are the simplest models to implement. However, a more accurate representation is desirable, since the electrostatic interaction has the largest magnitude and longest range of the intermolecular interaction energy components. Recent investigations suggest that simple atom-centered point charge representations of molecular charge distributions cannot provide an accurate description of the electrostatic potential at typical hydrogen-bonding distances.[21] Alternatives are partial charges distributed over many points, or multipolar expansions at several points. The distributed partial charge approach requires the optimization of both the charges and their positions by fitting quantum mechanically derived electrostatic potentials for prototypical spectator molecules. Various multicenter multipolar representations have been proposed which can be derived directly from the molecular wave function, and can form the basis of a relatively compact representation.[16,17,22–24] Many of these distributed multipolar analyses are related to atoms and bonds. This provides some hope for transferability from one system to another and the establishment of functional group libraries of representative electrostatic potentials.

The electrostatic interaction between the electronic distributions of an active molecule and a spectator can be evaluated from the quantum mechanical wave functions by

$$E_{AS}^{\mathrm{coul}} = -\int \Psi_A^*(i) V_S^{\mathrm{coul}}(i) \Psi_A(i) dr_i ,$$

$$V_S^{\mathrm{coul}}(i) = -\int \Psi_S^*(j) \frac{1}{r_{ij}} \Psi_S(j) dr_j , \tag{1}$$

where Ψ_A is the wave function of the active molecule and Ψ_S is the wave function of the spectator molecule. Following Buckingham,[20] if the charge distribution of the spectator is expanded in multipoles about an expansion point, C, and if the active and spectator species are not overlapping, the coulomb operator may be rewritten as a one-electron potential:

$$\begin{aligned} V_S^{\mathrm{coul}}(i) = & \sum_{x'}^{x,y,z} \left[\frac{N_S}{r_{iC}} \mu_{x'}^S F_{x'}(r_{iC}) \right] \\ & - \frac{1}{3} \sum_{x',x''}^{x,y,z} [\Theta_{x'x''}^S F'_{x'x''}(r_{iC})] \\ & - \frac{1}{15} \sum_{x',x'',x'''}^{x,y,z} [\Omega_{x'x''x'''}^S F''_{x'x''x'''}(r_{iC})] - \cdots , \end{aligned} \tag{2}$$

where N_S is the number of electrons in the spectator fragment, μ, Θ, and Ω are the dipole, quadrupole, and octupole moments, respectively, of the spectator fragment, and F, F', and F'' are the electric field, field gradient, and field second derivative operators (due to the active fragment) at the point C.

If the multipole expansion is carried out at a single point, the exact representation of the electrostatic potential of an arbitrarily shaped spectator molecule is slowly convergent. However, for a wave function expanded in a gaussian basis set, Rabinowitz, *et al.*[24] have shown that the electrostatic potential can be represented as a *distribution* of finite multipolar expansions centered at the origins of the gaussian primitive products that comprise an expansion of the molecular density. As shown by Boys,[25,26] any product of Gaussians is itself a Gaussian centered at an origin that is determined by the locations of the original Gaussians. The maximum order of the multipole expansion is the resultant angular momen-

This article is copyrighted as indicated in the article. Reuse of AIP content is subject to the terms at: http://scitation.aip.org/termsconditions. Downloaded to IP: 128.231.128.169 On: Mon, 07 Dec 2015 18:36:59

TABLE I. The multipolar electrostatic potential of formamide V_{mult} in kcal/mol/charge at selected points and the deviations from it using several more compact models.

Electrostatics Model	No. expan. points	Max. order of multipole	Selected points A	B	C	D	E
V_{mult}	288	3	51.66	37.90	−33.26	−70.51	−55.02
Atomic fitted	6	0	−7.20	0.28	−3.28	−5.54	12.09
multipoles	6	1	−4.86	−1.89	3.13	−1.46	−1.36
LMO multipoles	9	2	−1.58	12.16	11.56	8.57	−2.28
LMO multipoles	9	3	−1.95	18.27	14.57	8.65	−6.92
Atomic DMA	6	2	−4.70	2.90	−7.52	1.71	−3.66
(DMA1)	6	3	0.27	−0.84	0.78	−1.31	−1.22
Atoms+bonds	11	1	−23.70	−3.57	8.41	−22.29	12.28
DMA(DMA2)	11	2	−0.75	0.93	1.78	−0.39	1.20
DMA(DMA2)	11	3	−0.14	0.02	0.12	0.07	0.50

tum quantum number of the product Gaussian (e.g., $s=0$, $p=1$, $d=2$, etc.). This approach gives a finite exact expansion for a general *ab initio* density. However, for large basis sets and large collections of spectator molecules, this type of distributed expansion becomes unwieldy. So, it is useful to consider other, more compact, distributed multipolar expansions and compare these to the Rabinowitz expansion, V_{mult}. In Table I, some numerical values are presented for the electrostatic potential near the van der Waals envelope of the formamide molecule. The quantities were derived from a single configuration Hartree–Fock wave function[27] expanded in a compact effective potential, CEP-31G double-zeta basis set,[28] augmented with standard *d* polarization functions (exponent 0.8) on the non-H atoms.

Fitted partial charges, or charges and dipoles, located at the nuclei were obtained by an unweighted least squares fit to the *ab initio* potential on a diffuse grid of points.[29] The fitted potentials converge reasonably quickly, but there are indications that either atomic quadrupoles or additional expansion points may be required to achieve a uniform accuracy better than 1 kcal/mol/charge at van der Waals distances. The fitting procedure becomes more cumbersome for higher-order multipoles, and the optimized quantities are substantially dependent on the chosen grid.

A method proposed by Lavery *et al.*[30] for obtaining distributed multipolar expansions directly from localized molecular orbital (LMO)[26] densities is an attractive option, because it holds the promise of transferability from simpler to more complex systems, at least at the functional group level. The electron density of each LMO is used to generate a multipolar expansion at its centroid, or center of charge. However, the LMO multipolar expansions are not sufficiently converged (Table I), even at the octupole level, to guarantee high accuracy in the electrostatic potential at van der Waals distances.

Stone[16,17] has proposed the distributed multipolar analysis (DMA) method for obtaining distributed multipolar expansions. Like the Rabinowitz model, the DMA may be applied to any molecular density that is expanded in primitive Gaussian products, and it is not restricted to Hartree–Fock wave functions. The model consists of a user-defined set of centers about which subsets of densities from the molecular density matrix are expanded. For a Gaussian wave function, each Gaussian product density is expanded in multipoles at the DMA expansion center that is closest to its origin. For optimum convergence, the expansion centers are chosen so that densities are roughly localized and spherical around the assigned points. Stone *et al.*[17] have recommended using the atom positions and bond midpoints as expansion centers. The individual moments accumulated at an expansion point are basis set dependent, but the overall description of the molecular electrostatic potential is found to be quite acceptable. The Stone DMA analysis appears to give a well-converged representation of the electrostatic potential if the expansions are carried through quadrupoles and if both bond midpoints and atom positions are used as expansion centers. Octupole terms appear to be necessary if the expansion points are restricted to atom positions alone (denoted atomic DMA in Table I). Hydrogen atoms usually exhibit rapid multipole convergence. In Appendix A,[31] the formulas are given for the interaction energy of an *ab initio* charge distribution with a collection of multipole points carried out through octupoles.

The ease with which the DMA expansion may be obtained from any molecular wave function, and the accuracy of the DMA representation, make it the method of choice for all subsequent discussions in this work.

B. Charge penetration

The distributed multipolar expansion of a molecular electrostatic potential is convergent only at infinite distances from the molecule. At all other distances, the electronic contribution to the potential is affected by penetration of the molecular electron density. As a probe charge penetrates the electron density, interactions with the atomic nuclei become unshielded. For a neutral atom, the total electrostatic poten-

This article is copyrighted as indicated in the article. Reuse of AIP content is subject to the terms at: http://scitation.aip.org/termsconditions. Downloaded to IP: 128.231.128.169 On: Mon, 07 Dec 2015 18:36:59

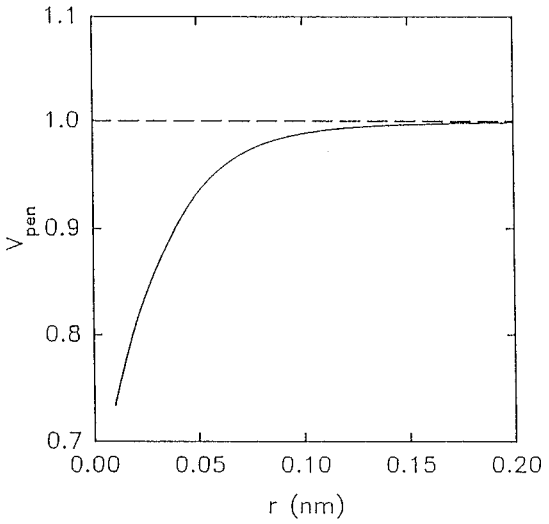

FIG. 1. Illustration of the penetration function in the electrostatic term [see Eq. (3)].

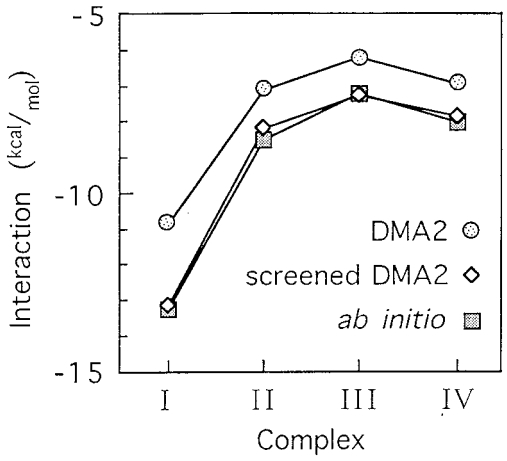

FIG. 2. Calculations of the interaction between formamide and water at the configurations of Fig. 5.

tial at a distance r from the nucleus, including charge penetration effects, can be represented simply by

$$V^{\mathrm{coul}}(r)=\frac{Z}{r}-\Phi^{\mathrm{pen}}(r)\,\frac{Z}{r}, \tag{3}$$

where Z is the atomic number and $\Phi^{\mathrm{pen}}(r)$ is a distance dependent multiplier that reduces the electronic contribution at finite distances. The first term in Eq. (3), the nuclear contribution, is exact at all distances for a point nucleus. The second term, the electronic contribution, must become exactly equal to the nuclear contribution as r approaches infinity for a neutral atom.

An example of the penetration function, Φ^{pen}, is shown in Fig. 1 for the electrostatic potential of the oxygen atom using a 6-31G[32] Hartree–Fock wave function. Since the penetration effect is fairly short-range, the molecular DMA approximation is accurate at van der Waals distances. However, when the DMA expansion is included in the Hamiltonian of an active molecule, the electron density penetrates close to the DMA expansion centers. Since the electrostatic interaction is an integral over the density as shown in Eq. (1), the penetration effect, if uncorrected, can be a source of substantial errors in the EFP. Since the nuclei of an active molecule do not approach the spectator too closely, the dominant effect of the penetration is in the electron–electron repulsion part of the interaction. Thus, the exact electrostatic interaction is always more attractive than the uncorrected DMA approximation.

The functional behavior exhibited in Fig. 1 suggests that a reasonable way to include these effects in the EFP model is to multiply each DMA expansion by an exponential cutoff, or ''screening'' function of the form

$$\Phi_k^{\mathrm{pen}}=1.0-c_k e^{-\alpha_k r^2}. \tag{4}$$

A Gaussian function has been chosen to simplify the integrals required for calculating the energy. The coefficients and exponents for each DMA center are optimized by fitting the exact *ab initio* electrostatic potential of a prototype molecule on a diffuse grid of points surrounding the molecule (see below). The effect of penetration[33] on the electrostatic interaction is illustrated in Fig. 2 for the formamide/water complex in four locally optimal hydrogen bonding orientations.[34] The Hartree–Fock molecular wave functions of the two molecules were calculated individually using CEP-31 G+d[28] basis sets. The *ab initio* Coulomb interaction between the molecules was evaluated using nonorthogonal molecular Hartree–Fock wave functions. In the DMA calculations, the water electron density was replaced by distributed multipolar potentials. The unscreened DMA results (Fig. 2) systematically underestimate the electrostatic attraction for all conformers by as much as 20%. Similar results have been found for many other complexes.[35] Multiplying each water DMA expansion by an optimized penetration function [Eqs. (3) and (4)] dramatically improves the agreement with the *ab initio* results (Fig. 2).

Other authors have discussed the importance of overlap and penetration effects in calculating electrostatic interactions. Ohta *et al.*[14] used a functional form similar to Φ^{pen} in their effective fragment potential method, but the screening is only indirectly involved in the important intermolecular interactions. Hall and co-workers[36] developed a method for fitting the compact parts of molecular electronic charge distributions while retaining the density matrix description of the most diffuse parts. This accounts for overlap penetration effects in electrostatic interactions in a qualitatively correct manner. We have found that the DMA method, when corrected for penetration effects, consistently reproduces *ab initio* intermolecular electrostatic interactions in the EFP method with errors $\leqslant 5\%$ at van der Waals distances, and with much smaller errors at longer distances. Thus, the radial and angular features of hydrogen bonding, which depend strongly on electrostatic interactions, can be reproduced accurately without introducing a semiempirical component. Other, more complex penetration functions have been tested, including nonspherical Gaussian functions and forms which

This article is copyrighted as indicated in the article. Reuse of AIP content is subject to the terms at: http://scitation.aip.org/termsconditions. Downloaded to IP: 128.231.128.169 On: Mon, 07 Dec 2015 18:36:59

include modification of the nuclear contribution to the potential. While these resulted in improvements in calculated energies in some cases, the simple single Gaussian cutoff model appears to be adequate for most EFP applications. More details are given in Appendix A.[31]

C. Interfragment interactions

If more than one spectator fragment is used, the electrostatic interactions between these fragments must be included in the model. Since the spectator fragments are modeled by multipolar expansions, simple classical interactions between these multipoles can be used in a manner consistent with the rest of the model, i.e., the point charges, dipoles, quadrupoles, and octupoles in each fragment will interact with those in the other fragments. For interfragment interactions both pieces need to be damped to account for charge penetration. The damping term can be thought of as spreading out the charge over a gaussian distribution, and the interaction energy can be obtained by integrating over these distributions. The result for the charge–charge interactions involves the error function. This and other details are given in Appendix B.[31]

III. POLARIZATION

Many analyses of hydrogen bonding interactions have shown that electronic polarization can contribute as much as 20% of the total interaction energy. In the EFP method, the polarization of the active molecules by the electric fields of the perturbing spectators occurs through the inclusion of perturber DMA electrostatic potentials in the active Hamiltonian. To model the polarization of the perturbers by the electric field of the active molecules, we introduce a set of spectator polarizabilities that interact with the active molecule electric fields. The induced moments that result from spectator polarization are then added to the active Hamiltonian, and these in turn repolarize the active molecule wave function. This process is iterated to self-consistency.

There are several possible functional representations of the spectator polarizabilities which have some analogy to the electrostatic potential representations discussed above. One possibility is to expand the interaction energy in terms of multipolar polarizabilities, hyperpolarizabilities, etc. as discussed by Buckingham:[20]

$$
\begin{aligned}
E^{\mathrm{pol}} = \sum_{x,x',x'',x'''}^{x,y,z} \Bigg\{ & -\frac{1}{2}\,\alpha_{xx'}F_xF_{x'} - \frac{1}{6}\,\beta_{xx'x''}F_xF_{x'}F_{x''} \\
& - \frac{1}{24}\,\gamma_{xx'x''x'''}F_xF_{x'}F_{x''}F_{x'''} - \frac{1}{3}\,A_{x:x'x''}F_xF'_{x'x''} \\
& - \frac{1}{6}\,B_{xx':x'''x''}F_xF_{x'}F'_{x''x'''} \\
& - \frac{1}{6}\,C_{xx':x'''x''}F'_{xx'}F'_{x''x'''} \Bigg\},
\end{aligned}
\tag{5}
$$

where α is the dipole polarizability tensor, β and γ are the first and second dipole hyperpolarizability tensors, and A, B, and C are the quadrupole polarizability tensors. Dykstra and co-workers[37] have developed methods to calculate molecular polarizabilities to any order. An alternative to this single-expansion-point approach is to use a distribution of point polarizabilities that may converge more rapidly and may respond more realistically to the spatially nonuniform fields that arise in molecular interactions. Van Duijnen and co-workers[8] have used distributed *atomic* polarizabilities in their structured reaction field work. However, such empirical polarizabilities are scalar quantities that cannot reproduce the polarization anisotropy associated with many molecules. The distributed polarization model developed by Stone[38] is rigorous and preferable in theory, but practical implementation problems limit it to systems characterizable by linear arrays of polarizable points.

For the EFP method, we use a distributed polarizability model based on bond and lone pair polarizabilities obtained from LMO, finite-field Hartree–Fock calculations.[26] Presently, only dipole polarizabilities are used, but, in principle, the method can be extended to any order of polarization. The polarizability tensors for representative spectator molecules are obtained as follows. Four self-consistent field (SCF) calculations are performed: one with no external perturbations and three with a small, uniform dipolar field term added to the one-electron Hamiltonian, oriented along one of three arbitrary cartesian coordinate axes. The Boys LMO's[26] from each of the converged finite-field SCF calculations are equivalent in structure to, but slightly perturbed from, the zero-field LMO's. For a closed-shell molecule, the total induced dipole moment (the difference in the dipole moment with and without the perturbing field) can be written as a sum of LMO components:

$$
\vec{\mu} = -2\sum_i \left[\langle \chi_i' | \vec{r} | \chi_i' \rangle - \langle \chi_i^0 | \vec{r} | \chi_i^0 \rangle\right], \tag{6}
$$

where χ^0 and χ' are the unperturbed and perturbed LMO's, respectively. An element of the polarizability tensor is related to the induced moment by

$$
\alpha_{xx'} = \lim_{F_{x'}\to 0} \frac{\mu_x}{F_{x'}} \tag{7}
$$

where F is the applied field and the x and x' subscripts refer to the cartesian components of the respective vectors. When the LMO expansion (6) is substituted for μ in Eq. (7), a decomposition of the total polarizability into LMO contributions is obtained:

$$
\begin{aligned}
\alpha_{xx'} &= \sum_i \alpha^i_{xx'} \\
&= -2\sum_i \lim_{F_{x'}\to 0}\left[\frac{\langle \chi_i' | r_x | \chi_i' \rangle - \langle \chi_i^0 | r_x | \chi_i^0 \rangle}{F_{x'}}\right].
\end{aligned}
\tag{8}
$$

Since the induced dipole moment is related to the shift in the centroids of the LMO's, the centroids are the natural origins for the LMO polarizability tensors. This is a well-behaved decomposition of the molecular polarizability. Unrealistically large positive or negative components are not

This article is copyrighted as indicated in the article. Reuse of AIP content is subject to the terms at: http://scitation.aip.org/termsconditions. Downloaded to IP: 128.231.128.169 On: Mon, 07 Dec 2015 18:36:59

found except in cases of high symmetry, for which the LMO centroid positions are not well determined. Special handling can resolve these cases satisfactorily. It is important to notice that while the total polarizability tensor for a molecule is symmetric, the same is not necessarily true for the individual LMO tensors. Therefore, all nine tensor components must be used in the polarization calculations. The correct variational form for the energy in the single fragment case has been derived in a manner analogous to the derivation by Karelson and Zerner[4] for the self-consistent reaction field energy.

The linear polarizability model (the induced dipole is assumed to be a linear function of the applied field) is used;

$$\vec{\mu}_i = \tilde{\alpha}_i \vec{F}_i . \tag{9}$$

In Eq. (9), $\vec{\mu}_i$ is the induced dipole vector at point i, $\vec{F}_i$ is the electric field vector at point i, and $\tilde{\alpha}_i$ is the corresponding polarizability tensor. In the current implementation of the effective fragment method, the number of induced dipoles included on each solvent molecule is determined by the number of valence molecular orbitals it has. An induced dipole is placed at the centroid of each localized molecular orbital in the valence shell. Thus, if the solvent is water, four induced dipoles are included for each solvent (fragment) molecule.

For just one fragment (solvent) molecule, the total change in energy of the system due to polarization is

$$E_{\mathrm{pol}} = E_{\mathrm{int}} + E_{\mathrm{sol}}, \tag{10}$$

E_{int} is the energy due to the interaction of the induced solvent molecule dipoles with the field,

$$E_{\mathrm{int}} = -\sum_i \vec{\mu}_i \cdot \vec{F}_i^{ai}, \tag{11}$$

where $\vec{F}_i^{ai}$ is the field at point i from the *ab initio* part of the system; E_{sol} is the energy required to induce the dipoles in the solvent molecule. E_{sol} has been shown[39] to be

$$E_{\mathrm{sol}} = \frac{1}{2}\sum_i \vec{\mu}_i \cdot \vec{F}_i^{ai} \tag{12}$$

when the linear polarizability model is used. Thus, the total polarization energy is

$$\begin{aligned} E_{\mathrm{pol}} &= -\sum_i \vec{\mu}_i \cdot \vec{F}_i^{ai} + \frac{1}{2}\sum_i \vec{\mu}_i \cdot \vec{F}_i^{ai} \\ &= -\frac{1}{2}\sum_i \vec{\mu}_i \cdot \vec{F}_i^{ai} = -\frac{1}{2}\sum_i (\tilde{\alpha}_i \vec{F}_i^{ai}) \cdot \vec{F}_i^{ai} . \end{aligned} \tag{13}$$

The field from the *ab initio* part can be written

$$\vec{F}_i^{ai} = \vec{F}_i^{\mathrm{nuc}} + \vec{F}_i^{\mathrm{el}} = \vec{F}_i^{\mathrm{nuc}} + \langle \psi | \vec{f}_i^{\mathrm{el}} | \psi \rangle, \tag{14}$$

where $\vec{F}_i^{\mathrm{nuc}}$ is the field from the nuclei in the *ab initio* part, $\vec{F}_i^{\mathrm{el}}$ is the contribution to the field from the electrons in the *ab initio* part, $\vec{f}_i^{\mathrm{el}}$ is the electronic field operator, and ψ is the electronic wave function. Thus, the polarization energy can be written,

$$E_{\mathrm{pol}} = -\frac{1}{2}\sum_i [\tilde{\alpha}_i (\vec{F}_i^{\mathrm{nuc}} + \langle \psi | \vec{f}_i^{\mathrm{el}} | \psi \rangle)] \cdot (\vec{F}_i^{\mathrm{nuc}} + \langle \psi | \vec{f}_i^{\mathrm{el}} | \psi \rangle). \tag{15}$$

The contribution from the solvent polarization energy to the Fock operator in the quantum mechanical self-consistent-field (SCF) procedure can be determined using the variational method. We form the functional

$$\begin{aligned} L = E_0 &- \frac{1}{2}\sum_i [\tilde{\alpha}_i (\vec{F}_i^{\mathrm{nuc}} + \langle \psi | \vec{f}_i^{\mathrm{el}} | \psi \rangle)] \cdot (\vec{F}_i^{\mathrm{nuc}} + \langle \psi | \vec{f}_i^{\mathrm{el}} | \psi \rangle) \\ &- W(\langle \psi | \psi \rangle - 1), \end{aligned} \tag{16}$$

where E_0 is the expectation value of H_0,

$$E_0 = \langle \psi | H_0 | \psi \rangle, \tag{17}$$

with H_0 being the Hamiltonian operator for the *ab initio* part plus the contributions from the other two parts of the effective fragment model, electrostatics and exchange repulsion. W in Eq. (16) is the Lagrange multiplier due to the normalization constraint. Variation of Eq. (16) with respect to wave function parameters gives

$$\begin{aligned} \delta L = \delta E_0 &- \frac{1}{2}\sum_i [(\tilde{\alpha}_i + \tilde{\alpha}_i^T)(\vec{F}_i^{\mathrm{nuc}} + \langle \psi | \vec{f}_i^{\mathrm{el}} | \psi \rangle)] \\ &\cdot \delta \langle \psi | \vec{f}_i^{\mathrm{el}} | \psi \rangle - W \delta \langle \psi | \psi \rangle \\ &= \langle \delta \psi | H_0 | \psi \rangle \\ &- \frac{1}{2}\sum_i [(\tilde{\alpha}_i + \tilde{\alpha}_i^T)(\vec{F}_i^{\mathrm{nuc}} + \langle \psi | \vec{f}_i^{\mathrm{el}} | \psi \rangle)] \\ &\cdot \langle \delta \psi | \vec{f}_i^{\mathrm{el}} | \psi \rangle - W \langle \delta \psi | \psi \rangle + cc = 0, \end{aligned} \tag{18}$$

where the superscript T denotes the matrix transpose and cc indicates the Hermitian conjugate of the preceeding expression. Thus, the Schrodinger equation for the state $|\psi\rangle$ is

$$\left(H_0 - \frac{1}{2}\sum_i [(\tilde{\alpha}_i + \tilde{\alpha}_i)(\vec{F}_i^{\mathrm{nuc}} + \langle \psi | \vec{f}_i^{\mathrm{el}} | \psi \rangle)] \cdot \vec{f}_i^{\mathrm{el}} \right) | \psi \rangle = W | \psi \rangle \tag{19}$$

or

$$\left(H_0 - \frac{1}{2}\sum_i (\vec{\mu}_i + \vec{\mu}_i^{\dagger}) \cdot \vec{f}_i^{\mathrm{el}} \right) | \psi \rangle = W | \psi \rangle, \tag{20a}$$

where

$$\vec{\mu}_i^{\dagger} = \tilde{\alpha}_i^T \vec{F}_i . \tag{20b}$$

The quantum mechanical energy obtained is thus

$$\begin{aligned} W &= \langle \psi | \left(H_0 - \frac{1}{2}\sum_i (\vec{\mu}_i + \vec{\mu}_i^{\dagger}) \cdot \vec{f}_i^{\mathrm{el}} \right) | \psi \rangle \\ &= E_0 - \frac{1}{2}\sum_i (\vec{\mu}_i + \vec{\mu}_i^{\dagger}) \cdot \langle \psi | \vec{f}_i^{\mathrm{el}} | \psi \rangle. \end{aligned} \tag{21}$$

The total energy of the system, obtained by adding E_{pol} to E_0, is

This article is copyrighted as indicated in the article. Reuse of AIP content is subject to the terms at: http://scitation.aip.org/termsconditions. Downloaded to IP: 128.231.128.169 On: Mon, 07 Dec 2015 18:36:59

TABLE II. Average magnitudes of the polarization energies E^{pol} (kcal/mol) and induced dipole moments μ^{ind} (Debye) for the distributed LMO polarizability method and the corresponding RMS *errors* for model results relative to SCF calculations. The structures are the four locally optimal *ab initio* formamide–water complexes (see Fig. 5).

		Average model		Average model	
	Induction model	E^{pol}	Error	μ^{ind}	Error
Polarizing formamide by water	Distributed LMO	−2.21	0.07	0.35	0.029
	One CM point		0.25		0.084
Polarizing water by formamide	Distributed LMO	−1.63	0.06	0.19	0.013
	One CM point		0.16		0.025

$$E = E_0 - \frac{1}{2}\sum_i \vec{\mu}_i \cdot (\vec{F}_i^{\mathrm{nuc}} + \langle \psi | \vec{f}_i^{\mathrm{el}} | \psi \rangle)$$

$$= E_0 - \frac{1}{2}\sum_i \vec{\mu}_i \cdot F_i^{\mathrm{nuc}} - \frac{1}{2}\sum_i \vec{\mu}_i \cdot \langle \psi | \vec{f}_i^{\mathrm{el}} | \psi \rangle$$

$$= W - \frac{1}{2}\sum_i \vec{\mu}_i \cdot \vec{F}_i^{\mathrm{nuc}} + \frac{1}{2}\sum_i \vec{\mu}_i^{\dagger} \cdot \langle \psi | \vec{f}_i^{\mathrm{el}} | \psi \rangle. \quad (22)$$

The last term in the final expression is the correction to the quantum mechanical energy, W, that is necessary in order to obtain the correct total energy. If the polarizability tensor is symmetric, this correction term is equivalent to the electronic part of E_{sol}, the energy required to polarize the solvent (fragment) molecule.

In the SCF iterations for the active-space wave function, the induced dipole moments are evaluated using the current values of the active space electric fields, and they are updated with each SCF iteration. So, the induced dipoles are made consistent with the active space wave function with little or no increase in the SCF computation time.

In calculating the induced dipoles in Eq. (9) there is no coupling of the induced moments within the spectator molecule, since the polarizability tensors were determined from fully coupled Hartree–Fock calculations. This is rigorous for a uniform dipolar perturbing field, but it is an approximation for the nonuniform fields encountered in molecular interactions. For systems with more than one spectator molecule, the induced moments within each molecule depend on the electric fields of the other spectators as well as the active part of the system, and the spectator–spectator polarization energy must be iterated to self-consistency.

In Table II we compare the polarization energy and induced dipole moment predicted by the distributed LMO polarizability model with Hartree–Fock results. *Ab initio* SCF calculations of the polarization of formamide by water and *vice versa* were carried out with one of the hydrogen-bonding partners replaced by a DMA expansion (uncorrected for penetration effects). Comparative classical calculations were then carried out with the *ab initio* molecule replaced by either distributed LMO point polarizabilities or a single point polarizability at the center-of-mass (CM). The distributed polarizability model reproduces the *ab initio* SCF polarization energy results and the induced dipole moments to within 10% or less. Note also that the polarization energy can be substantial and that both partners contribute to the total induction effect. Overall, the distributed LMO approach is energetically more accurate than the single CM polarizable point model.

When more than one solvent (fragment) molecule is included in the calculation, the interfragment interactions must be included in the polarizability energy. The induced dipole and the total polarization energy are still given by Eqs. (9) and (10), respectively, but, in this case, the expression for the interaction energy, Eq. (11), becomes

$$E_{\mathrm{int}} = -\sum_i \vec{\mu}_i \cdot \vec{F}_i^{ai} - \sum_i \vec{\mu}_i \cdot \vec{F}_i^{\mathrm{efp}} - \sum_i \sum_{j>i} \vec{\mu}_i \cdot \vec{F}_i^{\mu j}, \quad (23)$$

where $\vec{F}_i^{\mathrm{efp}}$ is the field at the polarizable point i due to the static multipoles in the other fragments, and $\vec{F}_i^{\mu j}$ is the field at point i from the induced dipole j, where j and i are not in the same fragment. The last term is the induced dipole-induced dipole interfragment interaction, and the sum over j is restricted to avoid double counting this interaction. Note that

$$\vec{\mu}_i \cdot \vec{F}_i^{\mu j} = \vec{\mu}_j \cdot \vec{F}_j^{\mu i}, \quad (24)$$

so that Eq. (23) can be written

$$E_{\mathrm{int}} = -\sum_i \vec{\mu}_i \cdot \vec{F}_i^{ai} - \sum_i \vec{\mu}_i \cdot \vec{F}_i^{\mathrm{efp}} - \tfrac{1}{2}\sum_i \vec{\mu}_i \cdot \vec{F}_i^{\mu}, \quad (25)$$

where

$$\vec{F}_i^{\mu} = \sum_j \vec{F}_i^{\mu j} \quad (26)$$

is the field at i from the induced dipoles in all the other fragments. The total field at i is given by

$$\vec{F}_i^{\mathrm{tot}} = \vec{F}_i^{ai} + \vec{F}_i^{\mathrm{efp}} + \vec{F}_i^{\mu} = \langle \psi | \vec{f}_i^{\mathrm{el}} | \psi \rangle + \vec{F}_i^{\mathrm{nuc}} + \vec{F}_i^{\mathrm{efp}} + \vec{F}_i^{\mu}, \quad (27)$$

so Eq. (25) can be written,

$$E_{\mathrm{int}} = -\sum_i \vec{\mu}_i \cdot \left(\vec{F}_i^{\mathrm{tot}} - \frac{1}{2}\vec{F}_i^{\mu} \right) \quad (28a)$$

$$= -\sum_i (\tilde{\alpha}_i \vec{F}_i^{\mathrm{tot}}) \cdot \left(\vec{F}_i^{\mathrm{tot}} - \frac{1}{2}\vec{F}_i^{\mu} \right) \quad (28b)$$

This article is copyrighted as indicated in the article. Reuse of AIP content is subject to the terms at: http://scitation.aip.org/termsconditions. Downloaded to IP: 128.231.128.169 On: Mon, 07 Dec 2015 18:36:59

$$= -\sum_i \left((\tilde{\alpha}_i \vec{F}_i^{\rm tot}) \cdot \vec{F}_i^{\rm tot} - \frac{1}{2} (\tilde{\alpha}_i^T F_i^{\mu}) \cdot \vec{F}_i^{\rm tot} \right) \tag{28c}$$

$$= -\sum_i \left(\vec{\mu}_i \cdot \vec{F}_i^{\rm tot} - \frac{1}{2} \vec{\mu}_i' \cdot \vec{F}_i^{\rm tot} \right) \tag{28d}$$

$$= -\sum_i \left(\vec{\mu}_i - \frac{1}{2} \vec{\mu}_i' \right) \cdot \vec{F}_i^{\rm tot}, \tag{28e}$$

where

$$\vec{\mu}_i' = \tilde{\alpha}_i^T \vec{F}_i^{\mu}. \tag{29}$$

Equation (12) in the multifragment case is

$$E_{\rm sol} = \frac{1}{2} \sum_i \vec{\mu}_i \cdot \vec{F}_i^{\rm tot} = \frac{1}{2} \sum_i \vec{\mu}_i \cdot (\langle \psi | \vec{f}_i^{\rm el} | \psi \rangle + \vec{F}_i^{\rm nuc} + \vec{F}_i^{\rm efp} + \vec{F}_i^{\mu}), \tag{30}$$

and the total polarization energy is

$$E_{\rm pol} = -\sum_i \vec{\mu}_i \cdot \left(\vec{F}_i^{\rm tot} - \frac{1}{2} \vec{F}_i^{\mu} \right) + \frac{1}{2} \sum_i \vec{\mu}_i \cdot \vec{F}_i^{\rm tot} \tag{31a}$$

$$= -\frac{1}{2} \sum_i \vec{\mu}_i \cdot (\vec{F}_i^{\rm tot} - \vec{F}_i^{\mu}) \tag{31b}$$

$$= -\frac{1}{2} \sum_i \vec{\mu}_i \cdot (\langle \psi | \vec{f}_i^{\rm el} | \psi \rangle + \vec{F}_i^{\rm nuc} + \vec{F}_i^{\rm efp}) \tag{31c}$$

$$= -\frac{1}{2} \sum_i (\tilde{\alpha}_i \vec{F}_i^{\rm tot}) \cdot (\vec{F}_i^{\rm tot} - \vec{F}_i^{\mu}) \tag{31d}$$

$$= -\frac{1}{2} \sum_i (\vec{\mu}_i - \vec{\mu}_i') \cdot \vec{F}_i^{\rm tot}. \tag{31e}$$

The next step, just as in the single fragment case, is to find the correct variational operator to include in the quantum mechanical self-consistent-field calculation. Equation (16) in the multifragment case is given by

$$L = E_0 - \frac{1}{2} \sum_i (\tilde{\alpha}_i \vec{F}_i^{\rm tot}) \cdot \vec{F}_i^{\rm tot} + \frac{1}{2} \sum_i (\tilde{\alpha}_i \vec{F}_i^{\rm tot}) \cdot \vec{F}_i^{\mu} - W(\langle \psi | \psi \rangle - 1). \tag{32}$$

Next, we need to take the variational of Eq. (32) with respect to wave function parameters. The only term in $\vec{F}_i^{\rm tot}$ with an explicit dependence on the wave function is the electronic term. The quantity $\vec{F}_i^{\mu}$ has an implicit dependence on the wave function, because it is a functional of induced dipoles which are dependent on the wave function. Since the induced dipoles are made self-consistent, this dependence is a second order effect and is ignored when taking the derivative. Thus, the variational equation is

$$\delta L = \delta E_0 - \frac{1}{2} \sum_i ([\tilde{\alpha}_i + \tilde{\alpha}_i^T] \vec{F}_i^{\rm tot}) \cdot \delta \langle \psi | \vec{f}_i^{\rm el} | \psi \rangle + \frac{1}{2} \sum_i (\tilde{\alpha}_i^T \vec{F}_i^{\mu}) \cdot \delta \langle \psi | \vec{f}_i^{\rm el} | \psi \rangle - W \delta \langle \psi | \psi \rangle$$

$$= \langle \delta\psi | H_0 | \psi \rangle - \sum_i \left(\frac{1}{2} \vec{\mu}_i + \frac{1}{2} \vec{\mu}_i^{\dagger} - \frac{1}{2} \vec{\mu}_i' \right) \cdot \langle \delta\psi | \vec{f}_i^{\rm el} | \psi \rangle - W \langle \delta\psi | \psi \rangle + cc = 0, \tag{33}$$

and the quantum mechanical energy is

$$W = \langle \psi | H_0 - \sum_i \left(\frac{1}{2} \vec{\mu}_i + \frac{1}{2} \vec{\mu}_i^{\dagger} - \frac{1}{2} \vec{\mu}_i' \right) \cdot \vec{f}_i^{\rm el}) | \psi \rangle = E_0 - \sum_i \left(\frac{1}{2} \vec{\mu}_i + \frac{1}{2} \vec{\mu}_i^{\dagger} - \frac{1}{2} \vec{\mu}_i' \right) \cdot \langle \psi | \vec{f}_i^{\rm el} | \psi \rangle. \tag{34}$$

Thus, in general, when there are any number of fragments, the total energy is calculated from the expression,

$$E = W - \frac{1}{2} \sum_i \vec{\mu}_i \cdot (\vec{F}_i^{\rm nuc} + \vec{F}_i^{\rm efp}) + \frac{1}{2} \sum_i (\vec{\mu}_i^{\dagger} - \vec{\mu}_i') \cdot \langle \psi | \vec{f}_i^{\rm el} | \psi \rangle. \tag{35}$$

The neglected terms in the EFP self-consistent polarization model include nonlinear polarizability terms, dispersion terms and more complex higher terms. The nonlinear polarizability may certainly be important in many applications, especially those involving charged species. Dispersion terms are presumed not to have important electronic structure effects. This is deduced from the known small values and R^{-7} distance dependence of dispersion-induced dipole moments. The energetics of dispersionlike interactions might be modeled by including R^{-6} terms as in many force field models, or by adjustment of the repulsive potentials discussed below.

IV. OVERLAP-DEPENDENT REPULSION

A. Exchange-orthogonality interactions

Strong repulsion between closed-shell molecules occurs when the electronic charge densities interpenetrate, in the presence of either attractive or repulsive electrostatic interactions. This phenomenon, which has no classical analog, is commonly known as the exchange-orthogonality interaction. The quantum mechanical origin and the magnitude of the exchange-orthogonality interaction has been discussed in detail by Morokuma and co-workers.[40] The dominant effect is that the charge density in the region of interpenetration is reduced below the sum of the densities of the unperturbed systems and increased elsewhere. This leads to a net repulsive interaction.[41]

If the supermolecule wave function, $\psi_{\rm AS}$, for two closed-shell molecules, A and S, is defined as a single product of the orthogonalized molecular wave functions, then the exchange-orthogonality interaction between A and S may be defined as

$$E_{AS}^{\rm exo} = \left[\frac{\langle \hat{A} \psi_A \psi_S | H | \hat{A} \psi_A \psi_S \rangle}{\langle \hat{A} \psi_A \psi_S | \hat{A} \psi_A \psi_S \rangle} - E_A - E_S \right] - E_{AS}^{\rm coul}, \tag{36}$$

where $\hat{A}$ is the antisymmetrizer, the term in brackets is the Heitler–London interaction, and $E_{AS}^{\rm coul}$ is the coulombic inter-

This article is copyrighted as indicated in the article. Reuse of AIP content is subject to the terms at: http://scitation.aip.org/termsconditions. Downloaded to IP: 128.231.128.169 On: Mon, 07 Dec 2015 18:36:59

action energy defined in Eq (1). The numerical value of E_{AS}^{exo} is dependent on the orientation of the two molecules, but independent of the orthogonalization method. Within this definition, it is straightforward to calculate the exchange–repulsion interaction between two molecular wave functions. Because of the electron permutation brought about by the antisymmetrizer, there is no simple local potential that can be used in the active molecule Hamiltonian to rigorously account for the exchange–repulsion interaction with the fragment.

B. Repulsive effective potentials

In the EFP method, the quantum mechanical exchange-orthogonality interaction, E_{AS}^{exo}, is modeled by simple repulsive effective potentials, V^{REP}, that are centered at specific points in the effective fragment molecules and included in the one-electron Hamiltonian of the active fragment. As outlined, it is possible to develop V^{REP} that either reproduce E^{exo} or which, when combined with the coulomb and polarization terms, reproduce the total quantum mechanical interaction energy between the active and effective fragment molecules. The former definition is used here.

The simplest model for repulsive interactions between the active and effective fragment molecules is

$$E_{AS}^{\mathrm{REP}}=\langle \psi_A | V_S^{\mathrm{REP}} | \psi_A \rangle, \tag{37}$$

where V_S^{REP} is a local one-electron operator positioned on the effective fragment molecule. The use of a local potential to model the nonlocal exchange-orthogonality interaction must be tested extensively, but similar approaches have been used quite successfully to model core/valence exchange-orthogonality interactions in atomic effective core potentials.[42]

The functional form of V_S^{REP}, and the method used to optimize the parameters depends on the definition of E_{AS}^{REP}. In most of the testing described here, E_{AS}^{REP} is taken as E_{AS}^{exo} [see Eq. (36)], which is evaluated using zeroth-order (unperturbed) active and spectator wave functions. A linear combination of Gaussian functions, centered on the effective fragment atomic nuclei, was chosen as a convenient representation of V_S^{REP}:

$$V_S^{\mathrm{REP}}=\sum_{i=1}^{N}\sum_{k=1}^{k_{\max}} c_{ik} G_{ik}(r_i), \tag{38}$$

where N is the number of atomic nuclei in the effective fragment molecule, and G is a simple spherical Gaussian, $\exp[-\alpha r^2]$. Angular factors can be introduced by using either cartesian Gaussians ($x^l y^m z^n \exp[-\alpha r^2]$) or Gaussian lobe functions with off-center expansions. One could also introduce multiplicative inverse powers of r as is done in the atomic effective core potentials.[42]

The Gaussian exponents, α_{ik}, and linear coefficients, c_{ik}, in Eq. (38) can be optimized to give the best fit of E_{AS}^{REP} to E_{AS}^{exo} for a collection of interacting geometries of A and S. For complex active and/or effective fragment molecules, functional-group-transferable parameters may be optimized for smaller prototypes, and the total V_S^{REP} taken as a sum of functional group potentials.

V. GEOMETRY OPTIMIZATIONS

A. Preliminary considerations

The quasi-Newton-Raphson optimization method in GAMESS[43] has been modified to include the solvent molecules, represented by effective fragments. Each solvent molecule is allowed to translate and rotate with fixed internal geometry. So each solvent molecule adds six degrees of freedom to the system. The optimization problem has $3n_a+6n_s$ total degrees of freedom, where n_a is the number of atoms in the solute molecule and n_s is the number of solvent molecules. Of these, 6 are the translational and rotational degrees of freedom of the entire system, $6n_s$ degrees of freedom are associated with the loose bonding (hydrogen bonding or van der Waals bonding) of the n_s solvent molecules to the solute molecule, and the remaining $3n_a-6$ are the vibrational degrees of freedom of the solute molecule.

The Newton–Raphson geometry search method is based on expanding the potential energy in a Taylor series, and truncating the series at quadratic terms.[44] In each step in the search, each atom is moved in the direction of the force on it according to

$$\mathbf{q}=\mathbf{H}^{-1}(\mathbf{x})\mathbf{F}(\mathbf{x}), \tag{39}$$

where $\mathbf{q}$ is the displacement vector from the coordinates given by the vector $\mathbf{x}$ to the new coordinates given by vector $\mathbf{x}_1$ ($\mathbf{q}=\mathbf{x}_1-\mathbf{x}$), $\mathbf{F}$ is the vector of the corresponding forces with components given by $F_i=-\partial E/\partial x_i$, and $\mathbf{H}$ is the Hessian, or second derivative matrix. E is the the potential energy function, i.e., the total energy of the molecule excluding nuclear kinetic energy. Since the surface is in general not quadratic, Eq. (39) is applied iteratively to find the minimum. The search method in GAMESS usually uses an approximate Hessian. When the exact Hessian is used to initiate the search, approximate updates are generally used in subsequent steps.

In geometry searches that include effective fragments, the contribution to the energy from the EFP changes the derivative of the energy with respect to the solute coordinates. In order to include the solvent (fragment) molecules in the geometry optimization, we need the forces on them, so we must calculate the energy derivative with respect to the coordinates of the fragment. The energy derivative has been derived with respect to each multipole expansion point, each polarizability point, and each exchange repulsion point. The first derivatives of the energy with respect to the effective fragment points cannot be used directly in the geometry search, however, because in the effective fragment model the internal geometry of the fragments is kept fixed, so we must constrain the points in a fragment from moving relative to each other. This is accomplished by combining the forces on the fragment to give a net force on the fragment and a net torque around the fragment molecule's center-of-mass. For each fragment, the three components of the net force and the

This article is copyrighted as indicated in the article. Reuse of AIP content is subject to the terms at: http://scitation.aip.org/termsconditions. Downloaded to IP: 128.231.128.169 On: Mon, 07 Dec 2015 18:36:59

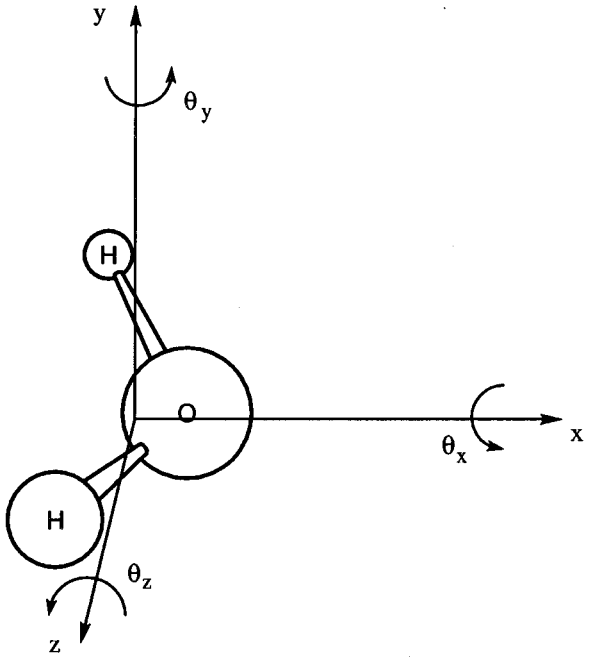

FIG. 3. The coordinates used to move the fragment in geometry optimizations.

three components of the net torque are included in the force vector, **F**, in Eq. (39). Three cartesian coordinates, representing the translational displacement of the fragment, are included in the displacement vector **q** in Eq. (39), corresponding to these three components of the net force. Three angles of rotation are included as components of **q** corresponding to the three components of the net torque. The coordinates used to displace the fragment molecule are shown in Fig. 3. The net force on a fragment is obtained by summing the forces on each fragment point; for example, the x component of the net force on fragment A is given by

$$F_{A,x}=\sum_{j}^{j\in A}\left(-\frac{\partial E}{\partial x_j}\right), \tag{40}$$

where j denotes a fragment point.

Calculation of the torque on the fragment is more complicated. The contribution to the torque from the interaction of nucleus N with the fragment monopole q is

$$\boldsymbol{\tau}_{Nq}=\mathbf{r}_q\times\mathbf{F}_{Nq}, \tag{41}$$

where $\mathbf{r}_q$ is a vector from the point of rotation (in this case the fragment center of mass) to the point of application of the force (the coordinates of monopole q), and $\mathbf{F}_{Nq}$ is the force vector for this interaction. However, the standard equation for the torque does not give the correct torque on dipoles and higher order multipoles when the force used is the derivative of the interaction energy. The derivative of a charge-dipole interaction energy, with respect to a coordinate of the dipole, gives the net force on the dipole, but this net force does not include all contributions to the net torque because a dipole may be thought of as two separated charges of equal magnitude and opposite sign. The net force on the dipole is the sum

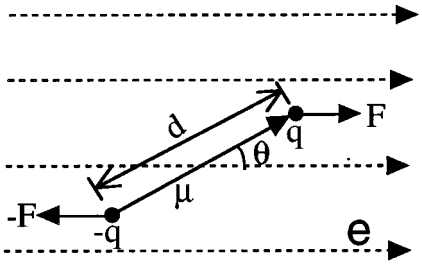

FIG. 4. A dipole of magnitude $\mu=qd$ placed in a uniform electric field of magnitude e.

of the forces on these two charges, so there is some cancellation of the forces in obtaining the net force. If the torque is calculated using Eq. (41) and this net force, the requirement that the net torque on the system be zero is not satisfied.

Figure 4 shows a dipole placed in a *uniform* electric field, $\boldsymbol{\epsilon}$. The net force on the dipole is zero, but there is a torque on the dipole in the direction perpendicular to the plane of the diagram and of magnitude $Fd\sin\theta=\boldsymbol{\epsilon}qd\sin\theta=\boldsymbol{\epsilon}\mu\sin\theta$. In vector form, this torque is given by[45]

$$\boldsymbol{\tau}=\boldsymbol{\mu}\times\boldsymbol{\epsilon}, \tag{42}$$

where $\boldsymbol{\mu}$ is the dipole moment vector. In the *nonuniform* field of an electric charge, the net force is not zero, but the term that is needed to correct the torque calculated by Eq. (41) is the torque given by Eq. (42), so the net torque on a dipole is given by

$$\boldsymbol{\tau}_{\mu}=\mathbf{r}\times\mathbf{F}+\boldsymbol{\mu}\times\boldsymbol{\epsilon}. \tag{43}$$

A charge Z produces an electric field Z/R^2 at a distance R. The Cartesian components of the electric field on a dipole from this charge are

$$\boldsymbol{\epsilon}_i=\frac{Zx_i}{R^3}, \tag{44}$$

where x_i is the ith cartesian coordinate. The formula for the correct torque on a quadrupole is

$$\boldsymbol{\tau}_{\Theta}=\mathbf{r}\times\mathbf{F}+\mathbf{Q}\times\mathbf{G}, \tag{45}$$

$$\mathbf{Q}=\Theta\mathbf{R}, \tag{46}$$

where Θ is the quadrupole matrix and the components of **R** are the Cartesian coordinates, x_i. The components of **G** are

$$G_i=\frac{Zx_i}{R^5}. \tag{47}$$

More explicit expressions for the additional terms in the torque are given in Appendix C,[31] including the correction to the torque on an octupole. The formulas for the torque corrections due to the interfragment electrostatic interactions are also given in Appendix C.[31] The total torque on a fragment is obtained by summing all these contributions to its torque from each of the fragment expansion points.

This article is copyrighted as indicated in the article. Reuse of AIP content is subject to the terms at: http://scitation.aip.org/termsconditions. Downloaded to IP: 128.231.128.169 On: Mon, 07 Dec 2015 18:36:59

B. Energy derivatives

1. Analytic gradients in ab initio calculations

The total energy of a molecule (excluding nuclear kinetic energy) is expressed in the molecular orbital (MO) basis as

$$E=\sum_i \sum_j \gamma_{ij}h_{ij}+\frac{1}{2}\sum_i \sum_j \sum_k \sum_l \Gamma_{ijkl}g_{ijkl}+V_{NN}. \tag{48}$$

V_{NN} is the nuclear repulsion energy, h_{ij} are one-electron Hamiltonian matrix elements, g_{ijkl} are two-electron matrix elements, γ_{ij} and Γ_{ijkl} are the one and two body density matrices, respectively, and i,j,k,l are MO labels. The corresponding expression in the atomic orbital basis (AO) is

$$E=\sum_p \sum_q d_{pq}h_{pq}+\frac{1}{2}\sum_p \sum_q \sum_r \sum_s D_{pqrs}g_{pqrs}+V_{NN}, \tag{49}$$

where d_{pq} and D_{pqrs} are the one and two body density matrices, respectively, and p,q,r,s are AO labels. The derivation of the gradient of E is well known,[46] so it is not repeated here. The resulting expression is

$$E^a=\sum_p \sum_q d_{pq}h^a_{pq}+\frac{1}{2}\sum_{pqrs} D_{pqrs}g^a_{pqrs}+V^a_{NN}-\sum_m \sum_i L_{mi}\sum_p \sum_q (c_{pi}S^a_{pq}c_{qj}), \tag{50}$$

where a superscript a indicates a derivative with respect to a nuclear coordinate x_a, c_{pi} is an AO to MO expansion coefficient, S_{pq} is an element of the AO overlap matrix, and L_{mi} is a Lagrangian multiplier;

$$L_{mi}=\left(\sum_j \gamma_{ij}h_{mj}+\sum_j \sum_k \sum_l \Gamma_{ijkl}g_{mjkl}\right). \tag{51}$$

2. Effective fragment contributions to the gradient

The expression for the energy given by Eq. (49) is modified to include the contributions from the effective fragments by making the substitutions

$$h_{pq}\rightarrow h_{pq}+V_{pq},$$

$$V_{NN}\rightarrow V_{NN}+V^{\mathrm{ef}}_N+V^{\mathrm{ef}}_{\mathrm{ef}},$$

where

$$V_{pq}=\langle\chi_p|\hat{V}^{\mathrm{ef}}|\chi_q\rangle.$$

$\hat{V}^{\mathrm{ef}}$ is the operator for the interaction between the fragment and the electron density, V^{ef}_N is the fragment-nucleus interaction energy, and $V^{\mathrm{ef}}_{\mathrm{ef}}$ is the fragment–fragment interaction energy. The corrected energy E' and energy gradient E'^a are

$$E'=E+\sum_p \sum_q d_{pq}V_{pq}+V^{\mathrm{ef}}_N+V^{\mathrm{ef}}_{\mathrm{ef}}, \tag{52}$$

$$E'^a=E^a+\sum_p \sum_q d^a_{pq}V_{pq}+\sum_p \sum_q d_{pq}V^a_{pq}+V^{(\mathrm{ef})a}_N+V^{(\mathrm{ef})a}_{\mathrm{ef}}. \tag{53}$$

The last term in Eq. (53), the contribution to the gradient due to the fragment–fragment interactions, is nonzero only when there is more than one fragment and when the derivative is with respect to a fragment coordinate. It is easily obtained since the terms contributing to the fragment–fragment interactions all have an analytic form with no dependence on the *ab initio* electron density. The formulas for the contributions to $V^{(\mathrm{ef})a}_{\mathrm{ef}}$ are given in Appendix B.[31]

The next-to-last term in Eq. (53), the contribution to the gradient due to the interaction of the effective fragment potential with the nuclei in the *ab initio* molecule, can be expressed as a sum of contributions from electric multipoles and polarization (V^a_{Np}),

$$V^{(\mathrm{ef})a}_N=V^a_{Nq}+V^a_{N\mu}+V^a_{N\Theta}+V^a_{N\Omega}+V^a_{Np}, \tag{54}$$

where multipoles through octupoles have been included. The expressions for the contributions to the derivative from the multipole-nuclei interactions and from the polarization-nuclei interactions with respect to the nuclear coordinates and with respect to the fragment coordinates are given in Appendix A.[31]

The third term in Eq. (53) can be written as:

$$\sum_p \sum_q d_{pq}V^a_{pq}=\sum_p \sum_q d_{pq}(\langle\chi^a_p|\hat{V}|\chi_q\rangle+\langle\chi_p|\hat{V}^a|\chi_q\rangle+\langle\chi_p|\hat{V}|\chi^a_q\rangle), \tag{55}$$

where χ_p is an atomic basis function. The first and third terms in Eq. (55) contain derivatives of the AO's and are treated in the usual manner.[46] When the derivative is with respect to a fragment coordinate, these terms are zero since the AO's do not depend on the fragment coordinates. The second term in Eq. (55) is zero if the derivative is taken with respect to the coordinates of the *ab initio* atoms since the fragment-electron interaction energy operator is independent of the nuclear coordinates. When the derivative is taken with respect to the coordinates of an effective fragment point, the operator has a mathematical form similar to that for the interaction between the fragment point and the nuclei. These terms are given for the monopole, dipole, quadrupole, octupole, polarization, and exchange repulsion terms in Appendix A.[31] The second term in Eq. (53) can be handled in the same way as the analogous term in the *ab initio* energy derivative, i.e., it is transformed into the last term in Eq. (50),

This article is copyrighted as indicated in the article. Reuse of AIP content is subject to the terms at: http://scitation.aip.org/termsconditions. Downloaded to IP: 128.231.128.169 On: Mon, 07 Dec 2015 18:36:59

which involves the derivative of the atomic overlap matrix. When the derivative is with respect to a fragment coordinate, this term will be zero since the AO's do not depend on the positions of the fragment coordinates. The term E^a, the derivative of the *ab initio* energy, will also be zero when x_a is a fragment coordinate. Thus, the derivatives with respect to a fragment coordinate and with respect to a coordinate of an *ab initio* atom become, respectively,

$$E'^a = V_{\mathrm{ef}}^{(\mathrm{ef})a} + V_N^{(\mathrm{ef})a} + \sum_p \sum_q d_{pq} \langle \chi_p | \hat{V}^a | \chi_q \rangle, \tag{56}$$

$$E'^a = E^a + \sum_p \sum_q d_{pq} (\langle \chi_p^a | \hat{V} | \chi_q \rangle + \langle \chi_p | \hat{V} | \chi_q^a \rangle) + V_N^{(\mathrm{ef})a}. \tag{57}$$

E^a is given by Eq. (50) but differs from the purely *ab initio* E^a because the electron-effective fragment interaction terms, V_{mj}, are included in the Lagrange multiplier matrix, and because the orbital coefficients have been changed by the presence of the effective fragment potential. Explicit expressions for the terms in the derivatives are given in Appendix A.[31]

The contribution to the energy gradient from the polarizability terms must be derived separately because the polarizability energy has a quadratic dependence on the charge density. In the following derivation, the coordinate x can be either one of the nuclear coordinates or one of the fragment coordinates.

Taking the derivative with respect to a coordinate x of the expression for the polarization energy in Eq. (15) gives a component of the energy gradient, i.e.,

$$\frac{\partial E_{\mathrm{pol}}}{\partial x} = -\frac{1}{2} \sum_i [(\tilde{\alpha}_i + \tilde{\alpha}_i^T)(\vec{F}_i^{\mathrm{nuc}} + \langle \psi | \vec{f}_i^{\mathrm{el}} | \psi \rangle)] \cdot \left(\frac{\partial \vec{F}_i^{\mathrm{nuc}}}{\partial x} + \frac{\partial}{\partial x} \langle \psi | \vec{f}_i^{\mathrm{el}} | \psi \rangle \right), \tag{58}$$

where the superscript T again denotes the matrix transpose. The derivative of the nuclear field is obtained easily from the formula for the electric field produced by a dipole. In the Hartree–Fock method, the wave function is expanded as a Slater determinant of MO's, ϕ_n,

$$\psi = |\phi_1 \phi_2 \cdots \phi_n\rangle, \tag{59}$$

and the MO's are expanded in AO's, χ_p, which are contracted Gaussian basis functions, i.e.,

$$\phi_n = \sum_p c_{pn} \chi_p. \tag{60}$$

Then, the expectation value of the electronic field operator is

$$\langle \psi | \vec{f}_i^{\mathrm{el}} | \psi \rangle = \sum_n \sum_m \gamma_{nm} (\vec{f}_i^{\mathrm{el}})_{nm} = \sum_p \sum_q d_{pq} (\vec{f}_i^{\mathrm{el}})_{pq}, \tag{61}$$

where γ_{nm} is the MO density matrix, d_{pq} is the AO density matrix, and $(\vec{f}_i^{\mathrm{el}})_{nm}$ and $(\vec{f}_i^{\mathrm{el}})_{pq}$ are the matrix elements of $\vec{f}_i^{\mathrm{el}}$ in the MO and AO basis, respectively. The derivative of this term is then

$$\frac{\partial}{\partial x} \langle \psi | \vec{f}_i^{\mathrm{el}} | \psi \rangle = \sum_p \sum_q \frac{\partial d_{pq}}{\partial x} (\vec{f}_i^{\mathrm{el}})_{pq} + \sum_p \sum_q d_{pq} \frac{\partial (\vec{f}_i^{\mathrm{el}})_{pq}}{\partial x}. \tag{62}$$

The second term in Eq. (62) must be evaluated using the chain rule to expand it into three terms. The methods for evaluating these terms are straightforward. When Eq. (62) is substituted into Eq. (58), the factor multiplied by the derivative of the density matrix is equal to the contribution to the Fock operator,

$$-\frac{1}{2} \sum_i (\vec{\mu}_i + \vec{\mu}_i^{\dagger}) \cdot \vec{f}_i^{\mathrm{el}},$$

Thus, this term is part of the Lagrange multiplier matrix and the entire term involving the density matrix derivative is transformed into a term involving the derivative of the overlap matrix.

In order to derive the expression for the contribution to the energy gradient from the polarization energy in the multifragment case, Eq. (31c) for the polarization energy is rewritten,

$$E_{\mathrm{pol}} = -\frac{1}{2} \sum_i [\tilde{\alpha}_i (\langle \psi | \vec{f}_i^{\mathrm{el}} | \psi \rangle + \vec{F}_i^{\mathrm{nuc}} + \vec{F}_i^{\mathrm{efp}} + \vec{F}_i^{\mu})] \cdot (\langle \psi | \vec{f}_i^{\mathrm{el}} | \psi \rangle + \vec{F}_i^{\mathrm{nuc}} + \vec{F}_i^{\mathrm{efp}}) \tag{63}$$

$$= -\frac{1}{2} \sum_i \left[\tilde{\alpha}_i \left(\sum_{pq} d_{pq} (\vec{f}_i^{\mathrm{el}})_{pq} + \vec{F}_i^{\mathrm{nuc}} + \vec{F}_i^{\mathrm{efp}} + \vec{F}_i^{\mu} \right) \right] \cdot \left(\sum_{rs} d_{rs} (\vec{f}_i^{\mathrm{el}})_{rs} + \vec{F}_i^{\mathrm{nuc}} + \vec{F}_i^{\mathrm{efp}} \right). \tag{63b}$$

This expression for the energy is expanded, and the gradient component is given by

This article is copyrighted as indicated in the article. Reuse of AIP content is subject to the terms at: http://scitation.aip.org/termsconditions. Downloaded to IP: 128.231.128.169 On: Mon, 07 Dec 2015 18:36:59

$$\frac{\partial E_{\rm pol}}{\partial x}=-\frac{1}{2}\sum_i\Bigg[\sum_{pqrs} d_{pq}d_{rs}((\tilde{\alpha}_i+\tilde{\alpha}_i^T)\vec{f}_i^{\rm el})_{pq}\cdot\frac{\partial(\vec{f}_i^{\rm el})_{rs}}{\partial x}+\sum_{pq} d_{pq}((\tilde{\alpha}_i+\tilde{\alpha}_i^T)\vec{f}_i^{\rm el})_{pq}\cdot\frac{\partial\vec{F}_i^{\rm nuc}}{\partial x}+\sum_{pq} d_{pq}((\tilde{\alpha}_i+\tilde{\alpha}_i^T)\vec{f}_i^{\rm el})_{pq}\cdot\frac{\partial\vec{F}_i^{\rm efp}}{\partial x}$$
$$+(\tilde{\alpha}_i+\tilde{\alpha}_i^T)\vec{F}_i^{\rm nuc}\cdot\sum_{pq} d_{pq}\frac{\partial(\vec{f}_i^{\rm el})_{pq}}{\partial x}+(\tilde{\alpha}_i+\tilde{\alpha}_i^T)\vec{F}_i^{\rm efp}\cdot\sum_{pq} d_{pq}\frac{\partial(\vec{f}_i^{\rm el})_{pq}}{\partial x}+(\tilde{\alpha}_i+\tilde{\alpha}_i^T)\vec{F}_i^{\rm nuc}\cdot\frac{\partial\vec{F}_i^{\rm nuc}}{\partial x}+(\tilde{\alpha}_i+\tilde{\alpha}_i^T)\vec{F}_i^{\rm efp}\cdot\frac{\partial\vec{F}_i^{\rm efp}}{\partial x}$$
$$+(\tilde{\alpha}_i+\tilde{\alpha}_i^T)\vec{F}_i^{\rm nuc}\cdot\frac{\partial\vec{F}_i^{\rm efp}}{\partial x}+(\tilde{\alpha}_i+\tilde{\alpha}_i^T)\vec{F}_i^{\rm efp}\cdot\frac{\partial\vec{F}_i^{\rm nuc}}{\partial x}+d_{rs}(\tilde{\alpha}_i+\tilde{\alpha}_i^T)(\vec{f}_i^{\rm el})_{rs}\cdot(\vec{f}_i^{\rm el})_{pq}\frac{\partial d_{pq}}{\partial x}+(\tilde{\alpha}_i+\tilde{\alpha}_i^T)\vec{F}_i^{\rm nuc}\cdot\sum_{pq}(\vec{f}_i^{\rm el})_{pq}\frac{\partial d_{pq}}{\partial x}$$
$$+(\tilde{\alpha}_i+\tilde{\alpha}_i^T)\vec{F}_i^{\rm efp}\cdot\sum_{pq}(\vec{f}_i^{\rm el})_{pq}\frac{\partial d_{pq}}{\partial x}\Bigg]-\frac{1}{2}\sum_i\tilde{\alpha}_i^T\Bigg(\sum_{pq} d_{pq}(\vec{f}_i^{\rm el})_{pq}+\vec{F}_i^{\rm efp}+\vec{F}_i^{\rm nuc}\Bigg)\cdot\frac{\partial\vec{F}_i^{\mu}}{\partial x}-\frac{1}{2}\sum_i\tilde{\alpha}_i\vec{F}_i^{\mu}\cdot\Bigg(\sum_{pq} d_{pq}\frac{\partial(\vec{f}_i^{\rm el})_{pq}}{\partial x}$$
$$+\sum_{pq}(\vec{f}_i^{\rm el})_{pq}\frac{\partial d_{pq}}{\partial x}+\frac{\partial\vec{F}_i^{\rm efp}}{\partial x}+\frac{\partial\vec{F}_i^{\rm nuc}}{\partial x}\Bigg). \tag{64}$$

The four terms in this expression containing the derivative of the density matrix can be written

$$-\frac{1}{2}\sum_i\Bigg\{(\tilde{\alpha}_i+\tilde{\alpha}_i^T)\Bigg[\sum_{rs} d_{rs}(\vec{f}_i^{\rm el})_{rs}+\vec{F}_i^{\rm nuc}+\vec{F}_i^{\rm efp}\Bigg]+\tilde{\alpha}_i\vec{F}_i^{\mu}\Bigg\}\cdot\sum_{pq}(\vec{f}_i^{\rm el})_{pq}\frac{\partial d_{pq}}{\partial x} \tag{65a}$$
$$=-\frac{1}{2}\sum_i\Bigg\{(\tilde{\alpha}_i+\tilde{\alpha}_i^T)\Bigg[\sum_{rs} d_{rs}(\vec{f}_i^{\rm el})_{rs}+\vec{F}_i^{\rm nuc}+\vec{F}_i^{\rm efp}+\vec{F}_i^{\mu}\Bigg]-\tilde{\alpha}_i^T\vec{F}_i^{\mu}\Bigg\}\cdot\sum_{pq}(\vec{f}_i^{\rm el})_{pq}\frac{\partial d_{pq}}{\partial x} \tag{65b}$$
$$=-\frac{1}{2}\sum_i\{(\tilde{\alpha}_i+\tilde{\alpha}_i^T)\vec{F}_i^{\rm tot}-\tilde{\alpha}_i^T\vec{F}_i^{\mu}\}\cdot\sum_{pq}(\vec{f}_i^{\rm el})_{pq}\frac{\partial d_{pq}}{\partial x} \tag{65c}$$
$$=-\sum_i\Bigg\{\frac{1}{2}\vec{\mu}_i+\frac{1}{2}\vec{\mu}_i^{\dagger}-\frac{1}{2}\vec{\mu}_i'\Bigg\}\cdot\sum_{pq}(\vec{f}_i^{\rm el})_{pq}\frac{\partial d_{pq}}{\partial x}. \tag{65d}$$

As in the single fragment case, this term is the contribution to the Fock operator multiplied by the density matrix derivative and therefore becomes part of the Lagrange multiplier matrix and is transformed into a term involving the overlap matrix derivative rather than the density matrix derivative. The rest of the terms in Eq. (64) can be written

$$\sum_i\Bigg\{-\frac{1}{2}(\vec{\mu}_i+\vec{\mu}_i^{\dagger})\cdot\Bigg[\sum_{pq} d_{pq}\frac{\partial(\vec{f}_i^{\rm el})_{pq}}{\partial x}+\frac{\partial\vec{F}_i^{\rm nuc}}{\partial x}+\frac{\partial\vec{F}_i^{\rm efp}}{\partial x}\Bigg]$$
$$+\frac{1}{2}\Bigg[\vec{F}_i^{\mu}\cdot\frac{\partial\vec{\mu}_i}{\partial x}-\Bigg(\sum_{pq}\frac{\partial d_{pq}}{\partial x}\tilde{\alpha}_i(\vec{f}_i^{\rm el})_{pq}\Bigg)\cdot\vec{F}_i^{\mu}-\vec{\mu}_i^{\dagger}\cdot\frac{\partial\vec{F}_i^{\mu}}{\partial x}\Bigg]\Bigg\}. \tag{66}$$

Evaluation of the terms in the first set of square brackets is straightforward. The formulas are obtained from Eqs. (A16) and (A22) in Appendix A[31] and Eqs. (B10), (B15), and (B16) in Appendix B.[31] Note that the field from the other induced dipoles is a linear combination of the other induced dipoles,

$$\vec{F}_i^{\mu}=\sum_{j^*}\tilde{k}_{ij}\vec{\mu}_j, \tag{67}$$

where the asterisk indicates that the sum is only over polarizable points j that are not part of the same fragment as point i, and each k_{ij} is a 3×3 matrix whose elements are given by Eq. (B19) in Appendix B.[31] So, the expression in the second set of square brackets in Eq. (66) can be written

$$\sum_i\sum_{j^*}\frac{1}{2}\Bigg[(\tilde{k}_{ij}\vec{\mu}_j)\cdot\frac{\partial\vec{\mu}_i}{\partial x}-(\tilde{k}_{ij}\vec{\mu}_j)\cdot\Bigg\{\tilde{\alpha}_i\sum_{pq}(\vec{f}_i^{\rm el})_{pq}\frac{\partial d_{pq}}{\partial x}\Bigg\}-\vec{\mu}_i^{\dagger}\cdot\frac{\partial(\tilde{k}_{ij}\vec{\mu}_j)}{\partial x}\Bigg] \tag{68a}$$
$$=\sum_i\sum_{j^*}\frac{1}{2}\Bigg[(\tilde{k}_{ij}\vec{\mu}_j)\cdot\frac{\partial\vec{\mu}_i}{\partial x}-(\tilde{k}_{ij}\vec{\mu}_j)\cdot\Bigg\{\tilde{\alpha}_i\sum_{pq}(\vec{f}_i^{\rm el})_{pq}\frac{\partial d_{pq}}{\partial x}\Bigg\}-\vec{\mu}_i^{\dagger}\cdot\Bigg(\frac{\partial\tilde{k}_{ij}}{\partial x}\vec{\mu}_j\Bigg)-\vec{\mu}_i^{\dagger}\cdot\Bigg(\tilde{k}_{ij}\frac{\partial\vec{\mu}_j}{\partial x}\Bigg)\Bigg] \tag{68b}$$
$$=\sum_i\sum_{j^*}\frac{1}{2}\Bigg[-\tilde{k}_{ij}\vec{\mu}_j\tilde{\alpha}_i\sum_{pq}(\vec{f}_i^{\rm el})_{pq}\frac{\partial d_{pq}}{\partial x}-\vec{\mu}_i\cdot\Bigg(\frac{\partial\tilde{k}_{ij}}{\partial x}\vec{\mu}_j\Bigg)\Bigg]. \tag{68c}$$

This article is copyrighted as indicated in the article. Reuse of AIP content is subject to the terms at: http://scitation.aip.org/termsconditions. Downloaded to IP: 128.231.128.169 On: Mon, 07 Dec 2015 18:36:59

If the polarizability tensors are symmetric, then $\vec{\mu}_i^{\dagger} = \vec{\mu}_i$, and since i and j sum over the same points, the first and last terms in expression (68b) cancel, yielding (68c). If the polarizability tensors are not symmetric, these two terms do not subtract out, and this method does not give an exact analytic gradient when there are multiple fragments. In practice, the polarizability contribution is small and this error in the gradient is not a severe limitation in geometry optimizations, but the use of symmetric polarizability tensors is recommended. The rest of this derivation assumes that the polarizability tensors are symmetric.

The last term in Eq. (68c) is identical to the gradient of the fixed dipole–dipole interaction energy, and could be evaluated either by Eq. (B15) or by using Eq. (B20) for $(\partial \tilde{k}_{ij})/(\partial x)$. The first term in Eq. (68c) can be written

$$\sum_i \sum_{j*} \frac{1}{2}\left[-\tilde{k}_{ij}\vec{\mu}_j\tilde{\alpha}_i\sum_{pq} d^a_{pq}(\vec{f}_i^{\,\mathrm{el}})_{pq}\right] = \sum_i \sum_{j*} \frac{1}{2}\left[-\tilde{k}_{ij}\vec{\mu}_j\tilde{\alpha}_i\sum_{pq}\left(\sum_r \sum_s c_{pr}\gamma_{rs}c_{qs}\right)^a(\vec{f}_i^{\,\mathrm{el}})_{pq}\right] \tag{69a}$$

$$= \sum_i \sum_{j*} \frac{1}{2}\left[-\tilde{k}_{ij}\vec{\mu}_j\tilde{\alpha}_i\sum_p \sum_q \sum_r \sum_s [c^a_{pr}\gamma_{rs}c_{qs}(\vec{f}_i^{\,\mathrm{el}})_{pq} + c_{pr}\gamma_{rs}c^a_{qs}(\vec{f}_i^{\,\mathrm{el}})_{pq}]\right]. \tag{69b}$$

The remainder of this derivation is closely related to that for the analogous term in the usual *ab initio* gradient and is omitted. In the RHF case, the expression in Eq. (69b) can be transformed into one involving the derivative of the atomic overlap matrix, and since the AO's are independent of fragment coordinates, it is zero. So, the first term in Eq. (68c) is zero, leaving just the second term of Eq. (68c) as the exact expression for the second line of Eq. (66).

VI. VIBRATIONAL ANALYSIS

The Hessian can be calculated numerically from the analytic first derivatives. When a numerically calculated Hessian is to be used for vibrational analysis, care must be taken to ensure that the analysis is accurate. In systems with nonbonded interactions, numerical Hessian calculations can give rise to qualitatively incorrect vibrational frequencies, due to the flatness of the surfaces in these systems. So, extra care should be taken in determining the stationary point geometry. If a numerical Hessian is to be used in the vibrational analysis, we recommend (a) all gradient components be reduced to 10^{-5} Hartree/bohr in the optimization step and (b) the use of points symmetrically displaced about the stationary point when evaluating numerical derivatives. It is also useful to use two sets of coordinates obtained with two different convergence criteria in two independent numerical hessian calculations for comparison. When fragment points are displaced, the two-electron integrals do not have to be recalculated. Note also that there are six displacements per fragment, independent of the number of points used to describe the potential.

VII. SAMPLE EFP CALCULATIONS

A. Water dimer

The effective fragment potential with the new optimization method described above is now applied to the water dimer system, where one water molecule is treated *ab initio* and the other water molecule is treated as an effective fragment. This system is small enough to allow comparison with full *ab initio* calculations on the water dimer system. Full *ab initio* geometry optimizations have been carried out on the water dimer at the Hartree–Fock level using (1) the Dunning–Hay (DH)[47] double-zeta basis, (2) the DH basis with *d* polarization functions on the O atoms, and (3) the DH basis with both *d* polarization functions on the O atoms and *p* polarization functions on the H atoms. The calculations are used for comparison to calculations in which one or the other of the water molecules has been replaced with an effective fragment.

The EFP used for the water molecule is described by five multipole expansion points, four polarization points, and three exchange repulsion points. The geometry of the fragment water molecule is fixed with bond lengths of 0.9572 Å and a bond angle of 104.52°. The multipole expansion points are located at the three nuclei and the two bond midpoints. Multipoles through octupoles, evaluated from *ab initio* calculations on the water molecule by the method described by Stone,[16,17] are included in the evaluation of the energy and its derivatives. The charges and the first, second, and third moments used in this work are given in Table III. The quadrupoles and octupoles are obtained from the second and third moments as described by Buckingham.[20] Four polarization points are used, located at the centroids of the four valence localized molecular orbitals. The polarizabilities, obtained from *ab initio* calculations carried out under the influence of an electric field, are also given in Table III. Three exchange repulsion points are included in the effective fragment potential, one located at each nucleus. The contribution to the interaction potential from each of these points is given by a sum of two Gaussians. The parameters in these Gaussian functions are also listed in Table III.

Since the two water molecules are not equivalent, the effective fragment method can be tested twice—first with the effective fragment replacing the water which is a hydrogen donor, and second with the effective fragment replacing the hydrogen acceptor water in the hydrogen bond. The water molecule not replaced with a fragment is treated in a full *ab initio* manner with each of the three basis sets listed above.

This article is copyrighted as indicated in the article. Reuse of AIP content is subject to the terms at: http://scitation.aip.org/termsconditions. Downloaded to IP: 128.231.128.169 On: Mon, 07 Dec 2015 18:36:59

TABLE III. The parameters defining the water effective fragment. The points O1, H3, and H4 denote the position of the oxygen atom and the two hydrogen atoms in the fragment. The points B13 and B14 are the midpoints of the bonds from the oxygen atom to H3 and H4, respectively. In the charge terms, the nuclear charge and the electronic charge have been included separately to allow the use of different screening parameters. The points with the nuclear charge are ZO1, ZH3, and ZH4. α is the exponential parameter in the screening factor and β is the pre-exponential factor.

Multipole coordinates, charges, and screening parameters.

Fragment point	X	Y	Z	Charge.	α	β
ZO1	−.582 78	2.209 67	.241 45	6.000 00	.502 21	10.092 72
ZH3	−.510 75	.4041 7	.158 28	1.000 00	.509 74	−4.496 13
ZH4	1.147 30	2.735 32	.191 78	1.000 00	.509 74	−4.496 13
O1	−.582 78	2.209 67	.241 45	−6.503 26	.499 26	9.179 11
H3	−.510 75	.404 17	.158 28	−.484 05	.510 19	−9.337 68
H4	1.147 30	2.735 32	.191 78	−.484 05	.510 19	−9.337 68
B13	−.546 76	1.306 92	.199 87	−.264 32	.490 97	1.462 34
B14	.282 26	2.472 49	.216 61	−.264 32	.490 97	1.462 34

Dipoles

Point	X	Y	Z
O1	.295 7	−.210 01	−.021 80
H3	−.002 70	−.000 95	.000 07
H4	.000 01	.002 86	.000 13
B13	−.035 52	.205 64	.010 62
B14	−.206 03	−.034 09	.007 18

Second moments

Point	XX	YY	ZZ	XY	XZ	YZ
O1	−4.159 61	−4.036 04	−4.842 82	.179 08	−.020 97	.028 34
H3	−.244 90	−.223 44	−.246 08	−.001 87	−.000 13	.001 09
H4	−.224 57	−.243 74	−.246 11	.005 21	−.000 68	−.000 11
B13	−.105 96	−.093 49	−.111 04	−.000 24	−.000 23	.000 79
B14	−.094 67	−.104 76	−.111 06	.003 69	−.000 53	.000 13

Third moments

Point	XXX	YYY	ZZZ	XXY	XXZ	XYY	YYZ	XZZ	YZZ	XYZ
O1	.885 50	−.594 52	−.069 93	−.256 07	−.022 04	.312 03	−.019 61	.316 26	−224 50	.001 14
H3	−.004 19	.030 28	.000 69	.004 34	.000 24	−.002 59	.001 12	−.001 51	.003 81	−.000 07
H4	−.029 30	−.000 58	.000 54	−.004 41	.000 70	−.005 67	.000 20	−.004 07	.000 18	.000 12
B13	−.118 54	.595 24	.031 53	.199 22	.010 40	−.040 30	.010 54	−.040 83	.197 99	−.000 03
B14	−.602 48	−.084 31	.021 85	−.027 00	.007 30	−.200 60	.007 08	−.200 54	−.026 57	.000 02

Polarizable points: coordinates and polarizabilities. The points are the centroids of the localized molecular orbitals.

Point	X	Y	Z	XX	YY	ZZ	XY	XZ	YZ	αP
LMO1	.372 69	2.481 35	.213 19	3.109 18	.694 80	.519 72	.719 24	−.077 50	−.022 46	.7
LMO2	−.525 40	1.218 67	.195 05	.509 06	3.290 34	.523 60	−.185 54	−.007 83	.131 06	.7
LMO3	−.803 17	2.358 92	.763 58	1.186 24	1.335 54	.769 42	.220 43	−.164 69	.127 16	.7
LMO4	−.845 73	2.403 68	−.245 05	1.212 93	1.354 52	.723 84	.197 57	.144 77	−.091 80	.7

Exchange repulsion points: coordinates and parameters. α_1 and α_2 are the exponential parameters and β_1 and β_2 are the pre-exponential factors.

Point	X	Y	Z	β_1	α_1	β_2	α_2
O1	−.582 78	2.209 67	.241 45	.062 22	.224 76	2.033 30	.517 65
H3	−.510 75	.404 17	.158 28	.002 06	.191 24	.084 65	.627 42
H4	1.147 30	2.735 32	.191 78	.002 06	.191 24	.084 65	.627 42

Its three atoms are allowed to relax to equilibrium without constraint. The internal structure of the effective fragment is kept fixed, but the fragment is allowed to translate and rotate toward a minimum energy configuration.

Table IV gives the geometric parameters of the equilibrium structure obtained in each type of calculation with the DH(d,p) basis (atoms 1–3 are in the donor). The most important geometric parameters in the effective fragment calculations are the internal coordinates of the *ab initio* molecule. These values are underlined in Table IV. The values marked with an asterisk are fixed in the effective fragment method. Table IV indicates that the internal structure of the ''solute'', or *ab initio*, water molecule is predicted quite accurately by the effective fragment method. In both effective fragment calculations, the bond lengths in the solute molecule agree with those from the full *ab initio* calculation to

This article is copyrighted as indicated in the article. Reuse of AIP content is subject to the terms at: http://scitation.aip.org/termsconditions. Downloaded to IP: 128.231.128.169 On: Mon, 07 Dec 2015 18:36:59

TABLE IV. Optimized geometries using the DH(d,p) basis. Interatomic distances in angstroms and angles in degrees. Italicized values are the values of most interest, i.e., the *ab initio* or solute, coordinates in an EF calculation. Values marked with *a* * were fixed by the EF method.

	Ab initio	Frag. H donor	Frag. H acceptor
r(O1–H2)	0.945	*0.944*	0.957*
r(O1–H3)	0.945	*0.944*	0.957*
r(O1–H5)	2.036	2.063	2.061
r(O4–H5)	0.949	0.957*	*0.948*
r(O4–H6)	0.943	0.957*	*0.943*
Angle(O4–H5–O1)	177.93	176.59	175.73
Angle(H2–O1–H5)	114.95	118.36	111.89
Dihedral angle (H2–O1–H5–O4)	−60.58	114.00	−58.43
Angle(H3–O1–H5)	115.00	118.36	111.89
Angle(H3–O1–H2	106.99	*106.99*	104.52*
Angle(H6–O4–H5)	106.52	104.52*	*106.52*
Dihedral angle (H6–O4–H5–O1)	180.00	0.00	180.00

within 0.001 Å, and the bond angle agrees to better than 0.01°. As for the relative positions of the two molecules, both of the effective fragment calculations predict a hydrogen bond length which is almost 0.03 Å (1.3%) longer than that in the full *ab initio* calculation. The orientation angles obtained in the effective fragment calculations are generally within 4° of those obtained in the full *ab initio* calculation.

Table V gives the interaction energies for the two water molecules at the equilibrium structures obtained from each of the three types of calculations with each of the three basis sets. In the calculations with the best basis set, DH(d,p), the interaction energies predicted by the H-donor EF calculation and by the H-acceptor EF calculation are less than the 5.0 kcal/mol predicted in the *ab initio* calculation by 0.5 kcal/mol and 0.3 kcal/mol, respectively. The effective fragment calculations actually have less basis set dependence than the *ab initio* calculations. Thus, when the smallest basis set is used, the results of EF calculations are closer to the best *ab initio* results than the smaller basis *ab initio* calculations. This is because the effective fragment potential has been fit to large basis set calculations, and this accuracy is reflected in the EF results even when a smaller basis is used. Note also that when either of the two larger basis sets is used, essentially the same interaction energy is obtained, regardless of which water molecule is represented by a fragment.

Table VI gives the harmonic vibrational frequencies and vibrational zero-point energies obtained at each minimum energy structure. Since only numerical hessians are available in effective fragment calculations, the accuracy of numerical

TABLE V. Interaction energies for water dimer (kcal/mol).

	DH	DH(d)	DH(d,p)
Full *ab initio*	−7.6	−5.3	−5.0
H donor replaced by eff. Frag.	−6.2	−4.7	−4.5
H acceptor replaced by eff. Frag.	−5.0	−4.7	−4.7

TABLE VI. Harmonic Frequencies (cm^{-1}) of water dimer obtained using the DH(d,p) basis. ff indicates that a mode was frozen by the effective fragment method.

	Ab initio		Fragment	
	Analytic	Numeric	H donor	H acceptor
1.	134	139	140	135
2.	144	148	155	147
3.	146	152	165	212
4.	170	172	173	217
5.	351	353	334	414
6.	614	615	543	658
7. H acceptor	1757	1757	1761	ff
8. H donor	1783	1783	ff	1791
9. H donor	4118	4118	ff	4135
10. H acceptor	4162	4162	4166	ff
11. H donor	4263	4263	ff	4268
12. H acceptor	4280	4280	4286	ff
Zero-point energy (kcal/mol)[a]	2.1	2.2	2.2	2.5

[a]This is the correction to the interaction energy due to the vibrational zero-point energy.

hessians was evaluated by computing the Hessian for the full *ab initio* system by both the analytic method and the numerical method. Since the minimum was located accurately (the convergence criteria required that the maximum component of the gradient be less than 10^{-6} Hartree/bohr) and since symmetrical displacements around the minimum of 0.001 Bohr were used in the numerical hessians, the agreement

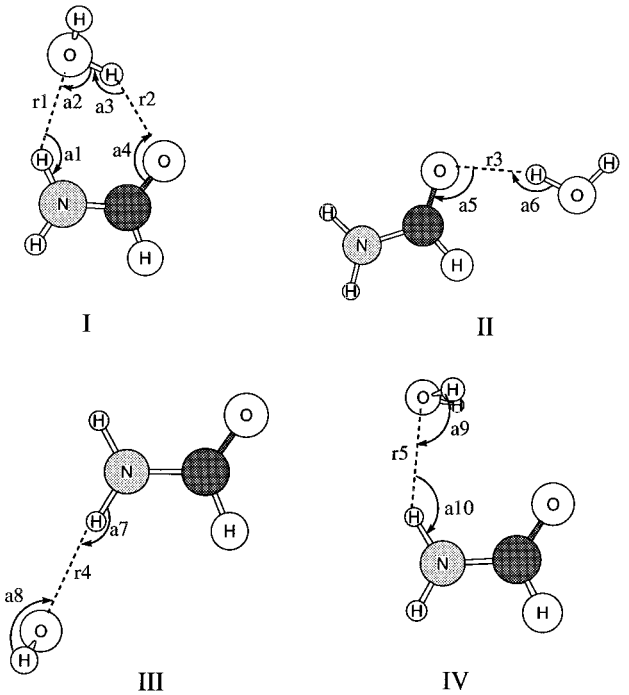

FIG. 5. Minimum energy configurations on the formamide–water potential energy surface, as obtained in full *ab initio* calculations with the DH(d,p) basis using C_1 symmetry. The geometrical parameters given correspond to the minima found by Jasien and Stevens using C_s symmetry. (a) structure I from Ref. 4, (b) structure II, (c) structure III, and (d) structure IV of Ref. 4, which is not a minima, but a saddle point.

This article is copyrighted as indicated in the article. Reuse of AIP content is subject to the terms at: http://scitation.aip.org/termsconditions. Downloaded to IP: 128.231.128.169 On: Mon, 07 Dec 2015 18:36:59

TABLE VII. Key geometrical parameters in optimized formamide–water structures. (All obtained with DZ(d,p)). The definition of each parameter is given in Fig. 5.

	Jasien and Stevens *ab initio* C_s (Ref. 9) sym.	*Ab initio* C_1 sym.	Effective fragment
I $r1$	2.161	2.195	2.248
I $r2$	2.061	2.053	2.219
I $a1$	138.6	138.6	141.5
I $a2$	83.7	80.5	82.0
I $a3$	143.3	146.6	140.5
I $a4$	110.1	109.8	110.2
II $r3$	2.029	2.013	2.060
II $a5$	118.8	104.7	122.4
II $a6$	169.0	155.0	178.7
III $r4$	2.121	2.100	2.136
III $a7$	175.9	175.0	176.4
III $a8$	178.5	180.0	147.5
IV $r5$	2.106	2.206	
IV $a9$	121.5	92.7	
IV $a10$	177.1	144.6	

between the analytic Hessian and the numerical Hessian is good. The six frequencies associated with the internal coordinates of the individual water molecules agree to better than 1 cm^{-1} between the two fully *ab initio* calculations, and the six frequencies associated with relative motion of the two molecules are higher in the numerical calculation than in the analytic calculation by 3.7%, 2.8%, 4.1%, 1.2%, 0.6%, and 0.2%, in order of increasing frequency. The harmonic analysis in the EF calculations shows an overestimation of the frequencies associated with the internal coordinates of the ''solute'' molecule by 0.2%, 0.1%, and 0.1% when the H donor is replaced with a fragment and by 0.4%, 0.4%, and 0.1% when the H acceptor is replaced with a fragment. For the frequencies associated with the relative motion of the two waters, the H-donor effective fragment calculation agrees quite well with the full *ab initio* calculation, except for the highest of these frequencies, for which the fragment result (543 cm^{-1}) is 12% less than the *ab initio* frequency. In the H-acceptor EF calculation, frequencies No. 3, 4, 5, 6 are up to 40% (for No. 3) higher than in the numerical *ab initio* calculation. This is the main reason that the adjustment to the vibrational zero-point energy is about 14% (0.3 kcal/mol) higher in this calculation than in the *ab initio* calculation. In contrast, the H-donor EF frequencies and zero-point correction agree quite well with the *ab initio* calculation.

B. Formamide–water

In order to evaluate the more general usefulness of the EFP for the water molecule, we need to study its interaction with solute molecules other than water. Formamide–water can be considered as a simple model for aqueous protein systems. In the *ab initio* study by Jasien and Stevens[34] four minima were found on the formamide–water potential energy surface, within the constraint of C_s symmetry. We have carried out *ab initio* geometry optimizations on this system with the water molecule replaced with an effective fragment. Since our EF calculations are done in C_1 symmetry, we have performed full *ab initio* geometry optimizations on this system using C_1 symmetry. The stationary point structures obtained in these full *ab initio* calculations [with the DH(d,p) basis] are shown in Fig. 5, and are labeled I–IV in correspondence to the minimum energy geometries given in Ref. 34. Table VII, compares the geometric parameters given in Ref. 34 for the relative orientation of the formaldehyde and water molecules at these minimum energy structures to the corresponding parameters obtained in this study, by both full *ab initio* calculations and by EF calculations. In the full *ab initio* calculations of this study, structure IV from Ref. 34

TABLE VIII. Internal coordinates of formamide molecule obtained in an *ab initio* calculation using the DH(d,p) basis, and the change in these coordinates caused by a hydrogen bonded water molecule, in configurations I, II, and III of Fig. 3. The changes are given as calculated both by the full *ab initio* method (a.i.) and by the effective fragment method (e.f.). Bond lengths are in angstroms and angles are in degrees.

	Formamide	I a.i.	I e.f.	II a.i.	II e.f.	III a.i.	III e.f.
r(C1–N3)	1.353	−0.009	−0.007	−0.006	−0.006	−0.005	−0.004
r(O2–C1)	1.196	0.009	0.007	0.007	0.004	0.004	0.004
r(H4–C1)	1.092	−0.002	−0.001	−0.003	−0.002	0.000	0.000
r(H5–N3)	0.995	0.005	0.005	0.000	0.000	0.000	−0.001
r(H6–N3)	0.992	0.000	0.000	0.000	0.000	0.005	0.004
Angle							
(N3–C1–O2)	124.9	000.2	000.2	−000.5	−000.3	000.5	000.5
(O2–C1–H4)	122.3	−001.0	−000.8	−000.4	−000.2	−000.3	−000.3
(N3–C1–H4)	112.8	000.8	000.6	000.9	000.5	−000.2	−000.2
(C1–N3–H5)	119.1	000.1	000.1	000.1	000.1	−000.5	−000.6
Dihedral							
(O2–C1–N3–H5)	000.0	001.6	002.6	000.4	−000.3	000.0	000.3
Angle							
(C1–N3–H6)	121.3	−000.7	−000.7	−000.1	−000.1	−000.1	−000.1
(H5–N3–H6)	119.6	000.6	000.4	000.0	000.0	000.6	000.7

This article is copyrighted as indicated in the article. Reuse of AIP content is subject to the terms at: http://scitation.aip.org/termsconditions. Downloaded to IP: 128.231.128.169 On: Mon, 07 Dec 2015 18:36:59

TABLE IX. Formamide–water interaction energies (Kcal/mol).

Structure	DZ–Jasien and Stevens *ab initio*, C_s	DH Fragment	DZ(d,p) Jasien and Stevens *ab initio*, C_s	DH(d,p) *ab initio*, C_1	DH(d,p) Fragment
I	−11.4	−7.5	−7.9	−8.3	−6.7
II	−8.0	−6.3	−5.8	−6.0	−5.1
III	−7.8	−5.1	−5.2	−5.3	−4.8
IV	−7.3		−5.2	−6.5[a]	

[a]This point is a saddle point, rather than a minimum. Since we did not do a saddle point search in the fragment calculations, this point was not found.

was found to be a saddle point rather than a minimum. Thus, this stationary point was not found in the EF calculations.

In the EF calculations on the three true minima, the length of the hydrogen bonds between the two molecules is longer than predicted by the *ab initio* calculations by just 0.04 ($r4$; 2%) to 0.17 ($r2$; 8%) Å. The orientational angles obtained in the EF calculations do not agree exactly with the *ab initio* calculations, but they are qualitatively correct. The geometric parameters of greatest interest, the internal coordinates of the formamide molecule, are compared in Table VIII. The first column in Table VIII lists the internal coordinates of a lone formamide molecule in its equilibrium configuration, as obtained in an *ab initio* calculation with the DH(d,p) basis, and the other six columns list the change in these coordinates caused by the presence of a water molecule. For each of the three minimum energy configurations, results are listed both from full *ab initio* calculations and from EF calculations. While the changes in these coordinates are small, the EF method consistently predicts nearly the same perturbation in these internal coordinates as was obtained in the full *ab initio* calculations.

Table IX lists the interaction energies obtained in Ref. 34 and in this study. For the three minima on the potential energy surface, the interaction energies obtained in the EF calculations at the DH(d,p) level differ from those from the full *ab initio* calculations with this basis by 1.6 (19%), 0.9 (15%), and 0.5 (9%) kcal/mol. Although the EF method underestimates the interaction energies, it does correctly predict that structure I is considerably more stable (by 1.6 kcal/mol, compared to 2.3 kcal/mol in the *ab initio* case) than structures II or III, and that structures II and III are comparatively close in energy. Also, as in the water dimer case, the EF calculation has less basis set dependence, and thus does better than *ab initio* at the double-zeta level, when compared to the larger *ab initio* calculations. The fact that the EFP method does not do quite as well at predicting the formamide–water interaction energy as it did at predicting the water dimer interaction energy may be due to the exchange repulsion part of the effective fragment potential, which was fit to the water dimer interaction. Considering this, the method does quite well. Since the formamide–water system is small enough to be treated in a full *ab initio* calculation, this system could in principle be used to construct an exchange repulsion potential that might be more accurate in modeling the hydration of amino acids and larger peptide systems.

TABLE X. Timing Information for geometry optimization of the water dimer using the DH(d,p) basis. All three of these used the same starting geometry, that obtained in a full *ab initio* optimization using a 3-21G basis.

	No. geometries	Total time (sec)	Time/geometry
Full *ab initio*	25	2516.2	100.6
H donor Eff. Frag.	21	440.8	21.0
H acceptor Eff. Frag.	18	372.5	20.7

C. Computational time savings

The goal of the EF method is to carry out calculations that would not be computationally feasible by full *ab initio* methods. The test cases considered in this study were chosen because they are small enough to be carried out by full *ab initio* methods, and thus can be used to judge the accuracy of the EF method. The savings in computational time that the method gives over full *ab initio* calculations is also of interest. Table X lists some computational timing information for minimum energy geometry searches on the water dimer system. Of greatest interest is the last column which gives the average computational time to evaluate the energy and gradient at one geometry. While the full *ab initio* calculation averaged just over 100 sec per geometry, the EF calculations required only about one fifth of this time. The EF method obtains its time savings by avoiding any two-electron integrals associated with the fragment molecule. Since the number of two-electron integrals tends to scale with the fourth power of the number of basis functions in an *ab initio* calculation, their evaluation becomes the limiting factor in calculations on larger systems. The time savings should be more dramatic when multiple fragments are included in EF calculations.

VIII. CONCLUSIONS

An effective fragment model has been developed to treat solvent effects on chemical properties and reactions, in such a manner that the solvent molecules are treated explicitly using a model potential that incorporates electrostatic, polarization, and exchange repulsion effects. The solute, which one can most generally envision as including some number of solvent molecules as well, is treated in a fully *ab initio* manner, using an appropriate level of electronic structure theory. In addition to the fragment model itself, formulae

This article is copyrighted as indicated in the article. Reuse of AIP content is subject to the terms at: http://scitation.aip.org/termsconditions. Downloaded to IP: 128.231.128.169 On: Mon, 07 Dec 2015 18:36:59

have been presented that permit the determination of analytic energy gradients and, therefore, numerically determined second derivatives. This will allow the method to be used to study the effect of solvents on molecular structures and vibrational frequencies, to analyze the effects of solvation on the nature and energetics of transition states, and to study solvent-modified reaction paths and, subsequently, dynamics.

The initial tests of the EFP method presented here are encouraging. The model appears to reproduce fully *ab initio* potentials well, and therefore to reproduce *ab initio* structures, energetics and vibrational frequencies to an acceptable level of accuracy. Subsequent tests of the method will address the possibility of developing transferable potentials so that many different solvents may be treated with a minimal effort, the importance of many body effects, and the applicability of the method to excited states and problems that involve multiple potential energy surfaces.

ACKNOWLEDGMENTS

This work was supported in part by grants from the Air Force Office of Scientific Research, the National Science Foundation, and the National Institute for Standards and Technology (to M.S.G.) and by Grant No. 88-00406 from the United States–Israel Binational Science Foundation (BSF), Jerusalem, Israel (to H.B.).

[1] L. Onsager, J. Am. Chem. Soc. **58**, 1486 (1936).
[2] O. Tapia and O. Goscinski, Mol. Phys. **29**, 1653 (1975).
[3] M. M. Karelson, A. R. Katritzky, M. Szafran, and M. C. Zerner, J. Org. Chem. **54**, 6030 (1989).
[4] M. M. Karelson and M. C. Zerner, J. Phys. Chem. **96**, 6949 (1992).
[5] M. Szafran, M. M. Karelson, A. R. Katritzky, J. Koput, and M. C. Zerner, J. Comp. Chem. **14**, 371 (1993).
[6] C. J. Cramer and D. G. Truhlar, in *Reviews in Computational Chemistry, Vol. 6*, edited by D. B. Boyd and K. B. Lipkowitz (VCH, New York, 1995); J. Tomasi and M. Persico, Chem. Rev. **94**, 2027 (1994); B. Honig, K. Sharp, and A.-S. Yang, J. Phys. Chem. **97**, 1101 (1993); M. E. Davis and J. A. McCammon, Chem. Rev. **90**, 509 (1990).
[7] U. C. Singh and P. A. Kollman, J. Comp. Chem. **5**, 129 (1984).
[8] B. T. Thole and P. T. Van Duijnen, Chem. Phys. **71**, 211 (1982); B. T. Thole and P. T. Van Duijnen, Theor. Chim. Acta **55**, 307 (1980).
[9] A. Warshel, J. Phys. Chem. **83**, 1640 (1979); A. Warshel and G. King, Chem. Phys. Lett. **121**, 124 (1985); G. King and A. Warshel, J. Chem. Phys. **91**, 3647 (1989); V. Luzhkov and A. Warshel, J. Am. Chem. Soc. **113**, 4491 (1991).
[10] M. J. Field, P. A. Bash, and M. J. Karplus, Comput. Chem. **11**, 700 (1990); J. Gao, J. Am. Chem. Soc. **116**, 1563 (1994); M. A. Thompson, E. D. Glendening, and D. F. Feller, J. Phys. Chem. **98**, 10465 (1994); F. Maseras and K. Morokuma, J. Comp. Chem. **16**, 1170 (1995).
[11] J. A. M. Romero and J. F. Sanz, J. Chem. Phys. **99**, 1255 (1993).
[12] J. H. Jensen, P. N. Day, M. S. Gordon, H. Basch, D. Cohen, D. R. Garmer, M. Krauss, and W. J. Stevens, in *Modeling the Hydrogen Bond*, edited by Douglas A. Smith, ACS Symposium Series 569, 1994, p. 139.
[13] W. Förner, P. Otto, J. Bernhardt, and J. J. Ladik, Theor. Chim. Acta **60**, 269 (1981).
[14] K. Ohta, Y. Yoshioka, K. Morokuma, and K. Kitaura, Chem. Phys. Lett. **101**, 12 (1983).
[15] A. H. de Vries, P. Th. van Duijnen, A. H. Juffer, J. A. C. Rullmann, J. P. Dijkman, H. Merenga, and B. T. Thole, J. Comput. Chem. **16**, 37 (1995).
[16] A. J. Stone, Chem. Phys. Lett. **83**, 233 (1981).
[17] A. J. Stone and M. Alderton, Mol. Phys. **56**, 1047 (1985).
[18] D. R. Garmer and W. J. Stevens, J. Phys. Chem. **93**, 8263 (1989).
[19] W. S. Stevens and W. H. Fink, Chem. Phys. Lett. **139**, 15 (1987).
[20] A. D. Buckingham, Quart. Rev. (London) **13**, 183 (1959).
[21] F. Colonna, E. Evleth, and J. G. Angyan, J. Comp. Chem. **13**, 1234 (1992); J. P. Ritchie and A. S. Copenhaver, J. Comp. Chem. **16**, 777 (1995); C. Chipot, J. G. Angyan, G. G. Ferenczy, and H. A. Scheraga, J. Phys. Chem. **97**, 6628 (1993).
[22] F. Vigne'-Maeder and P. Claverie, J. Chem. Phys. **88**, 4934 (1988).
[23] W. A. Sokalski and A. Sawaryn, J. Chem. Phys. **87**, 526 (1987).
[24] J. R. Rabinowitz, K. Namboodiri, and H. Weinstein, Int. J. Quantum Chem. **29**, 1697 (1986).
[25] S. F. Boys, Rev. Mod. Phys. **32**, 296, 300 (1960).
[26] S. F. Boys, in *Quantum Science of Atoms, Molecules, and Solids*, edited by P. O. Lowdin (Academic Press, NY, 1966), pp. 253–262.
[27] C. C. J. Roothaan, Rev. Mod. Phys. **23**, 69 (1951).
[28] W. J. Stevens, H. Basch, and M. Krauss, J. Chem. Phys. **81**, 6026 (1984); W. J. Stevens, H. Basch, M. Krauss, and P. Jasien, Can. J. Chem **70**, 612 (1992); T. R. Cundari and W. J. Stevens, J. Chem. Phys. **98**, 5555 (1993)
[29] D. E. Williams and J.-M. Yan, Adv. Atm. Mol. Phys. **23**, 87 (1988).
[30] R. Lavery, C. Etchebest, and A. Pullman, Chem. Phys. Lett. **85**, 266 (1982); C. Etchebest, R. Lavery, and A. Pullman, Theor. Chim. Acta (Berlin) **62**, 17 (1982).
[31] See AIP document no. PAPS JCPSA-105-1968-20 for 20 pages of Appendixes A, B, and C. Order by PAPS number and journal reference from American Institute of Physics, Physics Auxiliary Publication Service, Carolyn Gehlbach, 500 Sunnyside Boulevard, Woodbury, NY 11797-2999. Fax: 516-576-2223, e-mail: janis@aip.org. The price is $1.50 for each microfiche (98 pages) or $5.00 for photocopies of up to 30 pages, and $0.15 for each additional page over 30 pages. Airmail additional. Make checks payable to the American Institute of Physics.
[32] R. Ditchfield, W. J. Hehre, and J. A. Pople, J. Chem. Phys. **54**, 724 (1971); W. J. Hehre, R. Ditchfield, and J. A. Pople, J. Chem. Phys. **56**, 2257 (1972).
[33] The optimization of Φ^{pen} was determined using a uniform, rectangular grid of points surrounding the molecule in the exclusive volume between overlapping, concentric spheres with radii R_{min} and R_{max} centered at each atomic nucleus. To date, most fitting of Φ^{pen} has been for molecules containing just hydrogen, carbon, oxygen, and nitrogen atoms. Reasonable results have been obtained using R_{min}=1.5 bohr (0.08 nm) and R_{max}=4 bohr (0.21 nm) for hydrogen atoms and R_{min}=2.5 bohr (0.13 nm) and R_{max}=4.5 bohr (0.24 nm) for the other atoms. The accuracy of the results, and their dependence on the chosen radii does not warrant using unique radii for each type of nonhydrogen atom. Good potentials were obtained with this fitting method using around 50 grid points per atom.
[34] P. G. Jasien and W. J. Stevens, J. Chem. Phys. **84**, 3271 (1986).
[35] G. J. B. Hurst, P. W. Fowler, A. J. Stone, and A. D. Buckingham, Int. J. Quantum Chem. **29**, 1223 (1986).
[36] G. G. Hall, Adv. Atm. Mol. Phys. **20**, 41 (1985).
[37] C. E. Dykstra and P. G. Jasien, Chem. Phys. Lett. **109**, 388 (1984); C. E. Dykstra, J. Comp. Chem. **9**, 476 (1988).
[38] A. J. Stone, Mol. Phys. **56**, 1065 (1985).
[39] P. Debye, *Polar Molecules* (Dover, Mineola, NY, 1945), p. 30.
[40] K. Morokuma, J. Chem. Phys. **55**, 1236 (1971); K. Kitaura and K. Morokuma, Int. J. Quantum Chem. **10**, 325 (1976); K. Morokuma and K. Kitaura, in *Chemical Applications of Electrostatic Potentials*, edited by P. Politzer and D. G. Truhlar (Plenum, NY, 1981), pp. 215–242.
[41] L. Salem, Proc. Roy. Soc. (London) A **264**, 379 (1961).
[42] M. Krauss and W. J. Stevens, Ann. Rev. Phys. Chem. **35**, 357 (1984).
[43] M. W. Schmidt, K. K. Baldridge, J. A. Boatz, S. T. Elbert, M. S. Gordon, J. J. Jensen, S. Koseki, N. Matsunaga, K. A. Nguyen, S. Su, T. L. Windus, M. Dupuis, and J. A. Montgomery, J. Comput. Chem. **14**, 1347 (1993).
[44] J. D. Head and M. C. Zerner, Adv. Quantum. Chem. **20**, 1 (1988).
[45] See, for example, D. Haliday and R. Resnick, *Fundamentals of Physics* (J Wiley, New York, 1974), p. 443.
[46] P. Pulay, Mol. Phys. **17**, 197 (1969); Adv. Chem. Phys. **69**, 241 (1987).
[47] T. H. Dunning, Jr. and P. J. Hay, in *Methods of Electronic Structure Theory*, edited by H. F. Shaefer III (Plenum, NY 1977), pp. 1–27. Note that GAMESS uses inner/outer scale factors of 1.2 and 1.15 for DH's hydrogen. When polarization functions are added to this basis, the exponents used were 0.85 for the *d*-type functions on oxygen and 1.0 for the *p*-type functions on hydrogen.

This article is copyrighted as indicated in the article. Reuse of AIP content is subject to the terms at: http://scitation.aip.org/termsconditions. Downloaded to IP: 128.231.128.169 On: Mon, 07 Dec 2015 18:36:59